

A Field-Theoretical Paradigm via Hierarchical Coarse-Graining: I. Generalized Mode Theory

Jaehyeok Jin,^{1,2,#} Yining Han,^{1,#} and Gregory A. Voth^{1*}

¹Department of Chemistry, Chicago Center for Theoretical Chemistry, Institute for Biophysical Dynamics, and James Franck Institute, The University of Chicago, Chicago, IL 60637, USA

²Department of Chemistry, Columbia University, New York, NY 10027, USA

[#]Authors contributed equally

* Corresponding author: gavoth@uchicago.edu

Abstract

Multiscale computer simulations facilitate the efficient exploration of large spatiotemporal scales in chemical and physical systems. However, molecular simulations predominantly rely on particle-based representations, which become computationally prohibitive when applied beyond the molecular scale. Field-theoretical simulations have emerged as an alternative to overcome these limitations. Despite their applicability in mesoscopic simulations, these approaches are typically derived from top-down principles, leaving a gap in the bottom-up derivation of field-theoretical models for targeted molecular systems. This work presents a systematic strategy for constructing statistical field models for molecular liquids from the atomistic level, marking a critical step toward bridging particle-based and field-theoretical modeling techniques. By introducing molecular coarse-grained models as an intermediate step, this hierarchical approach reduces the complexity of the atomistic-to-field-theoretical transformation while preserving important microscopic structural correlations. We systematically derive field-theoretical models in reciprocal space for both canonical and grand canonical ensembles using the Hubbard-Stratonovich transformation. By incorporating additional fields for both positive and negative Fourier modes, our generalized mode theory extends the applicability of bottom-up field-theoretical models beyond the conventional Hubbard-Stratonovich transformation, which can be limited to positive Fourier modes. Furthermore, we introduce an efficient perturbative approach for approximating Fourier modes of molecular interactions, reducing computational cost and allowing for integrating complex molecular interactions into the field-theoretic description.

I. Introduction

In the study of molecular processes in chemical and physical systems, computer simulation has offered valuable insight along with efficiency and accuracy. Namely, atomistic particle-level simulations provide a molecular-level understanding of various chemical processes.¹⁻¹⁰ Extending the range of computer simulations to much longer time scales and larger length scales for complex molecular systems remains a challenging problem, yet “bottom-up” coarse-grained (CG) methodologies have been developed to address this issue by significantly reducing computational overheads.^{5, 8, 10-18} Instead of simulating the fully atomistic representation of systems, CG methodologies aim to construct a reduced particle resolution defined by mapping many degrees of freedom to fewer ones, such as capturing collective motions,¹⁹⁻²² charge,²³ symmetry,²⁴ etc. The effective CG interactions are then inferred from atomistic information, resulting in many-body CG potentials of mean force (PMFs).^{21, 22} Examples of these methodologies include inverse Monte Carlo (IMC),^{25, 26} iterative Boltzmann inversion (IBI),²⁷ relative entropy minimization (REM),²⁸⁻³⁰ and multiscale coarse-graining (MS-CG) (aka “force-matching”).^{19-22, 31} In turn, bottom-up CG models provide a reduced representation of underlying atomistic models, enabling exploration of much larger spatiotemporal scales.

While bottom-up CG approaches can extend the range of computer simulations while retaining physical accuracy, they are still constructed at the particle level. A particle-level representation inherently and eventually faces computational limitations when extended to much larger and longer scales. For molecular systems with relatively high resolution, where CG entities correspond to groups of spatially coherent fine-grained (all-atom) entities, these limitations may be less pronounced due to theoretical advances in CG modeling, e.g., Ultra-Coarse-Graining (UCG),³²⁻³⁷ as exemplified by recent studies in our group on virus capsid self-assembly.³⁸⁻⁴³ and quantum mechanics/CG molecular mechanics (QM/MM).⁴⁴⁻⁴⁶ However, this limitation becomes more pronounced at the mesoscopic and macroscopic levels beyond the micro-scales (i.e., μ s and μ m), where a specific CG entity may need to represent hundreds or even a much larger number of fine-grained degrees of freedom.⁴⁷⁻⁵⁸ The larger spatial scale smears out local correlations, resulting in a more smoothly varying spatial representation of the molecular system.⁵⁹⁻⁶⁴ In such situations, a particle-based theory may not be the most suitable choice for representing mesoscopic or macroscopic physics. This observation aligns with the current state of mesoscopic and macroscopic field-theoretical models.⁶⁴ For example, fluid mechanics and continuum mechanics theories are entirely constructed based on the field-theoretical description of fluids.⁶⁵ In equilibrium statistical mechanics, this approach is also widely used in liquid state theory⁶⁶⁻⁷⁴ and polymer physics.⁷⁵⁻⁸⁴

At this mesoscopic level and beyond, a set of field variables represents extremely coarsened objects, and their correspondence to the atomistic level is mostly not direct. Therefore, currently available field-theoretical models are primarily derived from phenomenological or top-down approaches such that the resultant model correctly represents experimental observables or captures the minimum physical behavior in a phenomenological manner.⁸⁵ However, the absence of microscopic origins in field-theoretical models poses limitations to our understanding of the underlying mechanisms can limit the accuracy and fidelity of these multiscale models. For example, many integral equation theories describing the liquid state⁶⁹⁻⁷³ have encountered challenges in capturing the complexity of homogeneous molecular liquids with irregular shapes

and complex orientational correlations. These challenges could be more pronounced when dealing with nanoscale heterogeneity, e.g., in ionic liquids.⁸⁶

In principle, an end goal of bottom-up coarse-graining could be to construct a well-defined field-theoretical model directly derived from an atomistic reference, with the capability to numerically sample the underlying fields. This two-part series of papers aims to develop bottom-up field theoretical coarse-graining methodologies, enabling the molecular nature to be incorporated into field-theoretical models under general ensemble conditions, including canonical and grand canonical ensembles. This framework, in principle, allows for capturing large-scale system conformations and morphologies while remaining extensible to heterogeneous multicomponent systems with distinct CG types and both inter- and intramolecular interaction terms. In addition, the grand canonical formulation enables efficient sampling of dense systems where particle-based insertion methods often encounter severe limitations.⁹ As the first step toward establishing this bottom-up connection, Paper I (this paper) focuses on developing a systematic bottom-up CG methodology that bridges the atomistic and mesoscopic field descriptions.

Microscopically deriving a field-theoretical representation from atomistic systems entails two major challenges: selecting appropriate field variables and statistically inferring field parameters across vastly different scales. To address these limitations, a more robust bottom-up theory capable of encompassing the diverse interaction characteristics of molecular systems is needed. Ideally, such a method should be directly derived from finer levels of description, specifically the atomistic level, to account for the complex nature of molecular interactions. However, transforming into field-theoretical representations presents significant practical challenges. First, the vast number of molecular degrees of freedom makes numerical implementation of such a field-theoretical approach computationally infeasible. Moreover, unlike conventional “particle” coarse-graining, a well-defined mapping from molecules to abstract fields and how to preserve microscopic information by condensing many orders of magnitude into a few field-theoretical model parameters become ambiguous. We therefore approach this challenge through a hierarchical framework. Rather than directly transforming the atomistic Hamiltonian into a field representation, we first introduce a molecular CG model as an intermediate step. By integrating out unnecessary “high frequency” degrees of freedom, this approach naturally resolves the computational challenges.

As our proposed hierarchical approach can help mitigate the statistical inference of the field Hamiltonian, the next critical task is to choose the correct field variables at the CG level that can accurately represent microscopic physics.⁸⁷⁻⁹⁰ Unlike conventional field-theoretical approaches that often define entirely new phenomenological fields (e.g., ϕ^4 theory⁹¹), the method pursued here directly translates a particle-based partition function into a field-based representation. In particular, our choice of a field variable is motivated by classical density functional theory (DFT) for liquids, where density variables are defined as microscopic density operators and play a central role in free energy functionals.^{92, 93} However, directly applying the density field variable requires additional determination of density functionals at the CG level.^{94, 95} Fortunately, the Fourier components of the density field naturally emerge in intermolecular interactions and the partition functions. Thus, it becomes natural to construct the field Hamiltonian from the reciprocal space of the molecular CG Hamiltonian. This hierarchical, density field-based approach simplifies the problem: Through coarse-graining, complex atomistic interactions involving numerous degrees of

freedom are reduced to effective interactions that are more tractable and involve significantly fewer degrees of freedom. In turn, constructing a bottom-up field-theoretical representation hinges on determining effective CG interactions and translating them into numerically field representations that can be sampled.

In the remainder of this paper, we develop the statistical mechanical theory using the auxiliary field method via a Hubbard-Stratonovich (HS) transformation.^{96, 97} In Sec. II, we formally introduce a hierarchical approach by presenting an “intermediate” molecular CG model to address bottlenecks in bottom-up, microscopically derived particle-to-field transformations. In Sec. III, we begin with the simplest case: the canonical partition function of a homogeneous system composed of a single molecule type, i.e., simple liquids, with all positive Fourier modes in the interaction. By carefully working out the HS transformation, we derive a classical field that governs the behavior of the underlying liquid. Section III C provides a bottom-up field representation of single-component systems. Next, in Sec. IV, we formalize the generalization of our approach to the grand canonical ensemble, incorporating fluctuations in particle number. In Sec. III D, we account for both positive and negative Fourier modes, addressing challenges in applying the conventional HS transformation to such cases. Finally, to enhance efficiency and address potential numerical issues, we explore perturbative approaches to approximate auxiliary fields in reciprocal space in Sec. V. As conventional perturbation theories for liquids are formulated in real space, we design several perturbative methods tailored to reciprocal space and evaluate their fidelity. Section VI concludes this Paper I. In closing this section, the central goal of Paper I is to extend the formal HS transformation to classical molecular systems by hierarchical coarse-graining, addressing complexities inherent to field-level interactions, and establishing a robust theoretical framework as the first step in this bottom-up methodology.

II. Hierarchical Coarse-Graining

While early studies aimed at establishing a microscopic-to-mesosopic correspondence have laid important groundwork, they were largely limited to simple interparticle interactions at the field-theoretical level. Most of these interactions were soft and analytical, including Yukawa,⁹⁸ Gaussian,⁹⁹⁻¹⁰² screened Coulombic,¹⁰³ or Morse potentials.¹⁰⁴ While the resulting field-theoretical models provided an analytical description of renormalized physics, these interactions were not representative of realistic microscopic physics, and, as a result, failed to fully capture the complex interaction nature of molecular systems. For example, in polymers,^{62, 63, 105} field-theoretical simulations often miss the underlying structures for copolymers due to the absence of microscopic physics.^{106, 107} To note, recent work done by Sherck et al.¹⁰⁸ on molecularly-informed field theories has aimed to bridge this gap between particle-level and field-level physics by applying the bottom-up coarse-graining on the basis of relative entropy minimization. While Ref. 108 and the subsequent studies to investigate large-scale coacervation and self-assembly behavior¹⁰⁹⁻¹¹¹ strongly suggest that microscopically-derived field-theoretical models can facilitate the understanding of multiscale phase behavior as a predictive tool, the effective interactions they employed remained limited to Gaussian interaction forms. Even though Gaussian core models can simulate polymeric behavior under specific conditions,¹¹² we suggest that this limited interaction form may still significantly hamper the potential of this field-theoretical approach to extend beyond certain polymeric interactions. This limitation becomes more apparent when dealing with

strong short-range repulsive behavior, e.g., in liquids¹¹³ or macromolecules with complex interaction profile beyond the expressivity of Gaussian.¹⁰

When incorporating molecular information into field-theoretical models, not only the ambiguities underlying the downfolding of numerous atomistic degrees of freedom, but more critically, conventional atomistic interactions, such as Coulombic and Lennard-Jones potentials, often diverge at short distances. As will be shown in Sec. III, these divergences render the Fourier transform ill-defined, preventing direct formulation at the density field level. This challenge is further compounded by the presence of multiple types of divergent interactions among different atoms. Recognizing that the correspondence between field-theoretical representations of molecular systems and the atomistic description remains largely unclear and unexplored. Here, Fig. 1 illustrates the proposed hierarchical CG approach from atoms to molecules, and then molecules to fields, in order to address some of these issues.

Using a bottom-up molecular-level CG methodology, the constructed molecular CG model captures essential correlations and interactions at this intermediate level. In particular, large wavenumber components at the atomistic resolution, which are prohibitively difficult to evaluate directly, are effectively smoothed out upon coarse-graining. From this reduced set of degrees of freedom, we proceed with mesoscopic coarse-graining to transition from the molecular CG level to the field-theoretical level, ultimately determining the field Hamiltonian of the microscopic system. This hierarchical coarse-graining approach is expected to more reliably describe complex liquid systems and recapitulate various correlations, offering a possibly significant advantage over *ad hoc* methods, which can at times fail to accurately capture microscopic correlations.

III. Field-Theoretical Transformation: Canonical Theory

To establish the framework, we begin with homogeneous, single-component molecular systems. While the initial focus is on single-component systems, we note that our theory is not limited to this scope. In Paper II, we will expand on these findings to generalize the approach for multi-component systems, thereby broadening the applicability of the proposed field-theoretical transformation.

A. Atomistic \rightarrow Molecular CG Level

We start with a finely detailed description of the target system of interest, i.e., the atomistic level. For molecules composed of n particles, the atomistic configurations are denoted as \mathbf{r}^n , and the corresponding atomistic interaction, $u(\mathbf{r}^n)$, is typically expressed in molecular mechanics as:

$$u(\mathbf{r}^n) = \sum_{nb} u_{nb}(\mathbf{r}^n) + \sum_b u_b(\mathbf{r}^n) + \sum_c u_c(\mathbf{r}^n), \quad (1)$$

where nb , b , and c represent non-bonded, bonded, and charged interactions, respectively. As previously discussed, the divergent repulsive terms prevalent in u_{nb} and u_c present significant challenges for deriving a well-defined effective field-theoretical transformation.

To resolve this challenge, we construct a molecular CG model from Eq. (1) with N CG particles (aka “beads”), where N is significantly smaller than n ($n \gg N$). For simplicity, in this work, we represent each CG liquid molecule by its center-of-mass, denoted as \mathbf{R}_I , which is determined by the mapping operator $\mathbf{M}(\mathbf{r}^n): \mathbf{r}^n \rightarrow \mathbf{R}^N$. Nevertheless, as we will discuss later in Subsection B, the

framework can readily accommodate multiple-site CG models without loss of generality. The effective CG interactions between these center-of-mass CG sites are assumed to be pairwise additive:

$$U(\mathbf{R}^N) = \frac{1}{2} \sum_{I \neq J} U(\mathbf{R}_I - \mathbf{R}_J), \quad (2)$$

where the pairwise CG potential $U(\mathbf{R}_I - \mathbf{R}_J)$ is only dependent on $R = |\mathbf{R}_I - \mathbf{R}_J|$. Comparing to Eq. (1), the relatively simple interaction form of Eq. (2), with fewer degrees of freedom, makes this approach advantageous for deriving the field-theoretical models. However, it is important to emphasize that the overall CG potential energy, $U(\mathbf{R}^N)$, should not be equated with the fine-grained (FG) internal energy $u(\mathbf{r}^n)$ from Eq. (1). Instead, $U(\mathbf{R}^N)$ approximates the FG free energy in the CG variables,¹⁹⁻²² accounting for the “missing entropy” effect.¹¹⁴⁻¹¹⁶ As demonstrated in particle-level coarse-graining, addressing the so-called *representability issue*¹¹⁷⁻¹²¹ will become critical for accurately estimating field-based properties, which will be further explored in Paper II.

The effective pairwise CG interaction $U(R)$ in Eq. (2) can be statistically inferred through various bottom-up coarse-graining methodologies. The main objective of bottom-up CG approaches is to determine effective equations of motion for the reduced representation that can capture important correlations at the CG level. Since forces are central to equilibrium equations of motion in both FG and CG variables, we adopt the MS-CG approach, which uses the force-matching methodology.^{19-22, 31} In MS-CG, $U(\mathbf{R}^N)$ is determined variationally by minimizing the force residuals, $\chi^2[\mathbf{F}]$, between the FG and CG systems:

$$\chi^2[\mathbf{F}] = \frac{1}{3N} \left\langle \sum_{I=1}^N |\mathbf{F}_I(\mathbf{M}(\mathbf{r}^n)) - \mathbf{f}_I(\mathbf{r}^n)|^2 \right\rangle, \quad (3)$$

where $\mathbf{F}_I(\mathbf{M}(\mathbf{r}^n))$ is the target CG force that is designed for matching the projected atomistic forces on the CG site I , containing atoms in the set \mathbb{I}_I , $\mathbf{f}_I(\mathbf{r}^n)$ is defined as $\mathbf{f}_I(\mathbf{r}^n) := \sum_{i \in \mathbb{I}_I} \mathbf{f}_i(\mathbf{r}^n)$. From the optimized pairwise force $\mathbf{F}_I(\mathbf{R}^N)$, the effective potential can be derived, as $\mathbf{F}_I(\mathbf{R}^N) = -\nabla_I U(\mathbf{R}^N)$. The pairwise forces obtained through this procedure satisfy the Yvon-Born-Green equation, thereby capturing up to three-body correlations.¹²² The MS-CG approach is particularly well-suited for hierarchical coarse-graining, as the primary focus here is on structural (static) correlations. For a more comprehensive review of bottom-up CG methodologies, the reader is referred to recent articles.^{17, 18}

Other than eliminating extraneous degrees of freedom and capturing important structures at the reduced level, introducing CG-level interactions in Eq. (1) simplifies complex atomistic interaction forms into additive CG pair interactions while alleviating divergent repulsions. As will be demonstrated in Subsection B, the large wavenumber (short-distance) features in the atomistic representation are typically smeared out in CG potentials,^{57, 58} making the HS transformation more feasible. Figure 1 illustrates this feature using the FG and CG potentials of an example liquid, CCl_4 , to demonstrate this feature (see Appendix B for computational details). In the conventional atomistic force field [here, Optimized Potential for Liquid Simulations (OPLS)^{123, 124}], the interactions underlying CCl_4 are categorized into two non-bonded interactions, two bonded interactions (bond and angle), and three charged interactions (C-C, C-Cl, and Cl-Cl). Since bonded

interactions often follow harmonic forms, we particularly focus on non-bonded and charged interactions, depicted in Figs. 1(a) and (b), respectively. These non-bonded and charged interactions are governed by the Lennard-Jones and Coulombic potentials, and hence diverge at zero distance. Therefore, a rigorous Fourier transformation cannot be applied because $\int_{r=0}^{r=\infty} d\mathbf{r} u_{\beta}(\mathbf{r}) \exp(-i\mathbf{k} \cdot \mathbf{r})$ (β : *nb* and *c*) is ill-defined at $u_{\beta}(r = 0)$ in the large wavenumber limit. However, as the $r = 0$ regime is not sampled in atomistic simulations, the effective molecular-level CG interactions derived from the atomistic statistics do not exhibit divergent repulsions at short distances. This observation is consistent with Fig. 1(c), where the bottom-up CG interactions are sampled only up to 4.02 Å and decay to zero at longer distances. While this also implies the absence of a continuous CG potential in the $r > 0$ domain, which cannot be directly Fourier-transformed, one can readily apply truncated or perturbation expansions to extrapolate this hard-core regime from the inferred CG interactions. This perspective will be further explored in Sec. V.

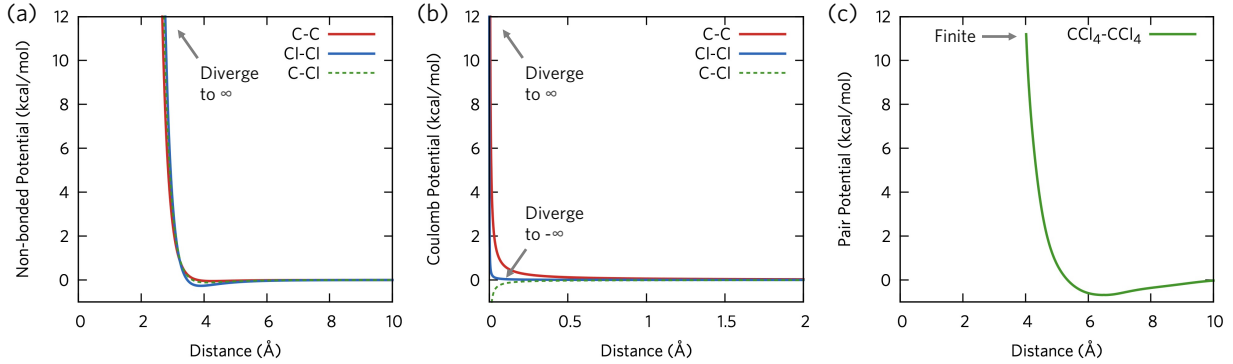


Figure 1. Divergent nature of conventional molecular mechanics force fields at the microscopic level, illustrated for CCl_4 at 300 K. (a) Non-bonded interactions between C and Cl pairs, represented by the Lennard-Jones potential. (b) Charged interactions between C and Cl pairs, described by the Coulomb potential. (c) The coarse-graining process mitigates these divergences by sampling non-divergent pair distances, as shown in the effective CG interactions.

With $U(R)$ well-defined at zero distance, the term $I = J$ can be included in the summation index in Eq. (2) as

$$U(\mathbf{R}^N) = \frac{1}{2} \sum_{I,J} U(\mathbf{R}_I - \mathbf{R}_J) - \frac{1}{2} N U(0). \quad (4)$$

Here, the self-interaction term $\frac{1}{2} N U(0)$ is introduced for notational consistency to correct the self-interaction term ($I = J$) and ensure the final form of $U(\mathbf{R}^N)$ only includes the terms from $\sum_{I \neq J} U(\mathbf{R}_I - \mathbf{R}_J)$. Combined with Eq. (3), Eq. (4) highlights the utility of hierarchical coarse-graining and serves as the starting point of the next coarse-graining step.

B. Molecular CG Level → Mesoscopic Field Level

Our next step is to transform this CG particle-based representation into a field representation. As mentioned in the Introduction, we do not specifically design microscopic field variables; instead, we utilize the density field operator, which naturally emerges in the reciprocal-space representation.

The microscopic density field operator and its Fourier transformation are rigorously defined, respectively, using delta functions, such that

$$\rho(\mathbf{R}) = \sum_{I=1}^N \delta(\mathbf{R} - \mathbf{R}_I), \quad (5a)$$

$$\rho(\mathbf{k}) = \int d\mathbf{R} \rho(\mathbf{R}) \exp(-i\mathbf{k} \cdot \mathbf{R}) = \sum_{I=1}^N \exp(-i\mathbf{k} \cdot \mathbf{R}_I), \quad (5b)$$

in which the \mathbf{k} vector denotes the reciprocal lattice vector that conforms to the periodic boundary conditions of the system of interest. Each component k_α (with $\alpha = x, y, z$) corresponds to discrete values defined by the periodic boundary conditions of a system with dimensions $L_x \times L_y \times L_z$, conforming to $k_\alpha = 2\pi n_\alpha / L_\alpha$, where n_α is an integer. The free energy function can be re-expressed in reciprocal space as follows, using the definition of the local density operator:

$$\begin{aligned} U(\mathbf{R}^N) &= \frac{1}{2} \int d\mathbf{R} d\mathbf{R}' \rho(\mathbf{R}) U(\mathbf{R} - \mathbf{R}') \rho(\mathbf{R}') - \frac{1}{2} N U(0) \\ &= \frac{1}{2} \int d\mathbf{R} d\mathbf{R}' \rho(\mathbf{R}) e^{i\mathbf{k} \cdot \mathbf{R}} \sum_{\mathbf{k}} U(\mathbf{k}) \rho(\mathbf{R}') e^{-i\mathbf{k} \cdot \mathbf{R}'} - \frac{1}{2} N U(0) \\ &= \frac{1}{2} \sum_{\mathbf{k}} \rho^*(\mathbf{k}) U(\mathbf{k}) \rho(\mathbf{k}) - \frac{1}{2} N U(0), \end{aligned} \quad (6)$$

where $\Sigma_{\mathbf{k}}$ is shorthand for summation over all reciprocal-space vectors $\mathbf{k} = (k_x, k_y, k_z)$.

In this reciprocal-space representation, we note that the free energy function can be represented as a quadratic function in terms of the Fourier modes of the density field operator. This quadratic form of Hamiltonian imparts a Gaussian structure to the partition function $[\exp(-\beta U(\mathbf{R}^N))]$, making it amenable to the well-known HS transformation⁹⁶ to transform the molecular CG partition function to a field representation,

$$\exp\left(-\frac{1}{2} a x^2\right) = \frac{1}{\sqrt{2\pi a}} \int dy \exp\left(-\frac{y^2}{2a} - ixy\right). \quad (7)$$

Here, a is a positive real constant. Notably, Eq. (7) effectively decouples pairwise intermolecular interactions from intramolecular (“bonded”) interactions, as the HS transformation applies specifically to terms involving $\rho^*(\mathbf{k}) U(\mathbf{k}) \rho(\mathbf{k})$. In typical CG models, bonded terms are often modeled as harmonic interactions (bonds, angles, and dihedrals) in the direct coordinate integral. These terms straightforwardly yield Gaussian integrals in the partition function, which remain unaffected by the transformation. For completeness, we provide an illustrative derivation of how bonded interactions can be handled for multiple-site CG models of liquids in Appendix A. This derivation gives the bond constraint analogous to the Gaussian chain term in polymer field theory.^{64, 125} While the main text primarily focuses on single-site CG models with no bonded terms for simplicity, our field-theoretical formulation of molecular CG partition functions is general and can accommodate multi-site CG representations.

The specific form of the HS transformation [Eq. (7)] also introduces two significant challenges when generalizing this approach to various molecular CG systems. First, the $a > 0$ condition limits the application of this transformation to CG interactions with positive Fourier modes. Since the interaction picture in reciprocal space differs from its real space counterpart (which is the target of most CG methodologies), this limit restricts the use of the HS transformation to a few analytical potentials with positive-definite Fourier modes. These examples include the Gaussian core model,¹²⁶ Yukawa,¹²⁷ or screened Coulomb¹²⁸ interactions. However, it is unlikely that the Fourier components of atomistically-derived CG interactions will always be positive. Second, $\exp(-ixy)$ in the integrand of the transformation is a complex number. When statistically evaluating such integrals using conventional numerical techniques, e.g., Monte Carlo sampling, it introduces a numerical phase problem (similar to sign problem¹²⁹⁻¹³¹ but more severe). These two factors have been critical bottlenecks in applying the bottom-up approach to design field-theoretical models. Here, we will first discuss the limited scenario where $\forall \mathbf{k}, U(\mathbf{k}) > 0$ and then generalize it to the case where $U(\mathbf{k})$ can take arbitrary values and signs. Additional numerical techniques to overcome the phase problem will be presented in Paper II.¹³²

Before elaborating on the field-level transformation, we note that our field-theoretical transformation differs slightly from the Self-Consistent Field Theory (SCFT) approach in that we do not invoke a microscopic delta functional $\delta[\rho - \hat{\rho}]$.⁶³ Moreover, our approach distinguishes itself from the methods taken by Efimov et al. in terms of the separation of variables.^{98-100, 102} A more comprehensive discussion on this will be provided in Paper II. Instead, our approach closely aligns with the field-theoretical transformation in Fourier space as introduced by Ref. 99. Nevertheless, as we will demonstrate in the remainder of this section, there are some factors that were unfortunately missing and overlooked in Ref. 99 during the HS transformation. Therefore, our aim is to provide a more correct and detailed derivation of the field-theoretical formulation for positive Fourier modes first in Subsection C (in a similar vein to what Ref. 99 attempted) and then extend this approach to the generalized modes in Subsection D (which was not covered in Ref. 99). Following this generalization, we will address how to overcome the phase problem associated with the auxiliary field.

C. Cases of Positive Fourier Modes

Under the pairwise approximation, the partition function of a molecular system in the canonical ensemble under constant NVT conditions, i.e., $Z(N, V, T)$, can be expressed as follows,

$$\begin{aligned} Z(N, V, T) &= \frac{1}{\lambda_B^{3N} N!} \int d\mathbf{R}^N \exp(-\beta U(\mathbf{R}^N)) \\ &= \frac{1}{\lambda_B^{3N} N!} \int d\mathbf{R}^N \exp\left(-\frac{1}{2}\beta \sum_{\mathbf{k}} \rho^*(\mathbf{k}) U(\mathbf{k}) \rho(\mathbf{k}) + \frac{1}{2}\beta N U(0)\right), \end{aligned} \quad (8)$$

in which λ_B represents the thermal de Broglie wavelength containing the momentum contribution in the form of Gaussian integrals. For the case when $\rho(\mathbf{k}) > 0$, we introduce an auxiliary field variable σ to perform the HS transformation to $Z(N, V, T)$. Before applying the HS transformation, we first introduce a set of properties for real field variables in configuration space denoted as $A(\mathbf{R})$, satisfying $A(-\mathbf{k}) = A^*(\mathbf{k})$. These properties will be of use in the later derivations for specific field variables $\sigma(\mathbf{R})$, $U(\mathbf{R})$, and $\rho(\mathbf{R})$:

$$\sum_{\mathbf{k} \neq 0} \sigma(\mathbf{k}) \rho^*(\mathbf{k}) = 2 \sum_{\mathbf{k} > 0} (\sigma^R(\mathbf{k}) \rho^R(\mathbf{k}) + \sigma^I(\mathbf{k}) \rho^I(\mathbf{k})), \quad (9a)$$

$$\sigma^*(\mathbf{k}) \sigma(\mathbf{k}) = \sigma^*(-\mathbf{k}) \sigma(-\mathbf{k}), \quad (9b)$$

$$\sum_{\mathbf{k} > 0} \frac{1}{U(\mathbf{k})} \sigma^*(\mathbf{k}) \sigma(\mathbf{k}) = \frac{1}{2} \sum_{\mathbf{k} \neq 0} \frac{1}{U(\mathbf{k})} \sigma^*(\mathbf{k}) \sigma(\mathbf{k}). \quad (9c)$$

The HS transformation begins with the observation that the quadratic term in Eq. (6), except $\rho^*(\mathbf{k} = 0)U(\mathbf{k} = 0)\rho(\mathbf{k} = 0)$, can be grouped as

$$\begin{aligned} \sum_{\mathbf{k} \neq 0} \rho^*(\mathbf{k}) U(\mathbf{k}) \rho(\mathbf{k}) &= \sum_{\mathbf{k} < 0} \rho^*(\mathbf{k}) U(\mathbf{k}) \rho(\mathbf{k}) + \sum_{\mathbf{k} > 0} \rho^*(\mathbf{k}) U(\mathbf{k}) \rho(\mathbf{k}) \\ &= \sum_{\mathbf{k} > 0} |\rho(-\mathbf{k})|^2 U(-\mathbf{k}) + \sum_{\mathbf{k} > 0} |\rho(\mathbf{k})|^2 U(\mathbf{k}) = \sum_{\mathbf{k} > 0} |\rho(\mathbf{k})|^2 [U(-\mathbf{k}) + U(\mathbf{k})] \\ &= 2 \sum_{\mathbf{k} > 0} |\rho(\mathbf{k})|^2 \text{Re}\{U(\mathbf{k})\}, \end{aligned} \quad (10)$$

due to $U(-\mathbf{k}) = U^*(\mathbf{k})$ for real-space pair potentials. Equation (10) suggests that only the real part of the Fourier transform of the pairwise interaction contributes to the total energy. Therefore, we define the real part $\phi(\mathbf{k}) := \text{Re}\{U(\mathbf{k})\}$, which is assumed to be positive in this case. Then, we observe that the exponential part contains two Gaussian contributions from the real part $\rho_R(\mathbf{k})$ and the imaginary part $\rho_I(\mathbf{k})$ of the Fourier modes of the density operator:

$$\begin{aligned} \exp\left(-\frac{1}{2}\beta \sum_{\mathbf{k} \neq 0} \rho^*(\mathbf{k}) U(\mathbf{k}) \rho(\mathbf{k})\right) \\ = \exp\left(-\beta \sum_{\mathbf{k} > 0} |\rho(\mathbf{k})|^2 \phi(\mathbf{k})\right) = \exp\left(-\beta \sum_{\mathbf{k} > 0} (\rho_I(\mathbf{k})^2 + \rho_R(\mathbf{k})^2) \phi(\mathbf{k})\right). \end{aligned} \quad (11)$$

Therefore, the HS transformation of the non-zero Fourier component involves auxiliary variables for $\rho_R(\mathbf{k})$, denoted as $\xi(\mathbf{k})$, and for $\rho_I(\mathbf{k})$, denoted as $\eta(\mathbf{k})$. Then, two HS transformations can be written as

$$\begin{aligned} \exp\left(-\frac{1}{2}\beta \sum_{\mathbf{k} \neq 0} \rho^*(\mathbf{k}) U(\mathbf{k}) \rho(\mathbf{k})\right) \\ = \prod_{\mathbf{k} > 0} \frac{1}{4\pi\beta\phi(\mathbf{k})} \int \prod_{\mathbf{k} > 0} d\xi(\mathbf{k}) d\eta(\mathbf{k}) \exp\left[-\sum_{\mathbf{k} > 0} \frac{1}{4\beta\phi(\mathbf{k})} (\xi(\mathbf{k})^2 + \eta(\mathbf{k})^2) \right. \\ \left. - i \sum_{\mathbf{k} > 0} [\zeta(\mathbf{k}) \rho^*(\mathbf{k})]\right]. \end{aligned} \quad (12)$$

Instead of introducing two variables, for notational convenience, these two auxiliary fields can be compactly represented as a single complex (auxiliary) field $\zeta(\mathbf{k}) := \xi(\mathbf{k}) + i\eta(\mathbf{k})$. Then, since the local density field $\rho(\mathbf{R})$ is a real field variable, there is an additional condition that ξ and η should satisfy, i.e., $\zeta(\mathbf{k}) = \zeta^*(-\mathbf{k})$. Now, we further simplify the functional form of Eq. (12). From Eq. (9), the last term in Eq. (12) becomes $i \sum_{\mathbf{k}>0} \zeta(\mathbf{k}) \rho^*(\mathbf{k}) = i \sum_{\mathbf{k}>0} (\rho_R(\mathbf{k}) \xi(\mathbf{k}) + \rho_I(\mathbf{k}) \eta(\mathbf{k}))$, and $\prod_{\mathbf{k}>0} 1/4\pi\beta\phi(\mathbf{k}) = \prod_{\mathbf{k}\neq 0} \sqrt{1/4\pi\beta\phi(\mathbf{k})}$, since $\phi(\mathbf{k}) = \phi(-\mathbf{k})$ by definition. Therefore, we can absorb the factor of 2 into the integration variable to reduce the exponential integrand in the partition function into the following form.

$$\begin{aligned} & \exp\left(-\frac{1}{2}\beta \sum_{\mathbf{k}\neq 0} \rho^*(\mathbf{k}) U(\mathbf{k}) \rho(\mathbf{k})\right) \\ &= \prod_{\mathbf{k}\neq 0} \left[2 \sqrt{\frac{1}{\pi\beta\phi(\mathbf{k})}} \right] \int \prod_{\mathbf{k}>0} d\frac{\xi(\mathbf{k})}{2} d\frac{\eta(\mathbf{k})}{2} \exp\left[-\sum_{\mathbf{k}>0} \frac{1}{\beta\phi(\mathbf{k})} \left\{ \left(\frac{\xi(\mathbf{k})}{2}\right)^2 + \left(\frac{\eta(\mathbf{k})}{2}\right)^2 \right\} \right. \\ & \quad \left. - 2i \sum_{\mathbf{k}>0} \left[\rho_R(\mathbf{k}) \left(\frac{\xi(\mathbf{k})}{2}\right) + \rho_I(\mathbf{k}) \left(\frac{\eta(\mathbf{k})}{2}\right) \right] \right] \end{aligned} \quad (13)$$

Now, we define the final auxiliary field variable in a complex vector form $\sigma(\mathbf{k}) := \sigma_R(\mathbf{k}) + i\sigma_I(\mathbf{k})$, where $\sigma_R(\mathbf{k}) = \xi(\mathbf{k})/2$ and $\sigma_I(\mathbf{k}) = \eta(\mathbf{k})/2$, that also satisfies $\sigma(\mathbf{k}) = \sigma^*(-\mathbf{k})$. The final result reads as

$$\begin{aligned} & \exp\left(-\frac{1}{2}\beta \sum_{\mathbf{k}\neq 0} \rho^*(\mathbf{k}) U(\mathbf{k}) \rho(\mathbf{k})\right) \\ &= \prod_{\mathbf{k}\neq 0} \left[2 \sqrt{\frac{1}{\pi\beta\phi(\mathbf{k})}} \right] \int \prod_{\mathbf{k}>0} d\sigma_R(\mathbf{k}) d\sigma_I(\mathbf{k}) \exp\left[-\frac{1}{2} \sum_{\mathbf{k}\neq 0} \frac{\sigma(\mathbf{k}) \sigma^*(\mathbf{k})}{\beta\phi(\mathbf{k})} \right. \\ & \quad \left. - i \sum_{\mathbf{k}\neq 0} [\sigma(\mathbf{k}) \rho^*(\mathbf{k})] \right]. \end{aligned} \quad (14)$$

Note that the last two summations in the exponential function are changed from $\sum_{\mathbf{k}>0}$ to $\sum_{\mathbf{k}\neq 0}/2$ as per Eq. (9). In this final expression, it is important to emphasize that our formulation differs from the equation initially presented in Ref. 99 by a factor of 2 for each reciprocal lattice vector. This underscores the necessity for a careful HS transformation on two separate field variables. For canonical systems, the zero wave vector contribution does not need the HS transformation, since $\rho(\mathbf{k}=0) = N$ is a fixed value. Therefore, its contribution to the partition function is just $\exp\left[-\frac{\beta}{2} \phi(\mathbf{k}=0) N^2\right]$. Since $\phi(\mathbf{k}=0)$ is constant given the interaction potential, this will not enter through the action functional (which only contains $\mathbf{k} \neq 0$ contributions in canonical cases).

Finally, the complete form of a canonical partition function [Eq. (8)] is expressed as an integral of two auxiliary fields as

$$\begin{aligned}
\mathcal{Z}(N, V, T) &= \frac{1}{\lambda_B^{3N} N!} \int d\mathbf{R}^N \exp \left[\frac{1}{2} N \beta U(0) \right] \exp \left[-\frac{\beta}{2} \phi(\mathbf{k} = 0) N^2 \right] \prod_{\mathbf{k} \neq 0} \left(\frac{4}{\pi \beta \phi(\mathbf{k})} \right)^{\frac{1}{2}} \\
&\times \int \prod_{\mathbf{k} > 0} d\sigma_R(\mathbf{k}) d\sigma_I(\mathbf{k}) \exp \left[-\frac{1}{2} \sum_{\mathbf{k}} \frac{\sigma^*(\mathbf{k}) \sigma(\mathbf{k})}{\beta \phi(\mathbf{k})} - i \sum_{\mathbf{k}} \sigma(\mathbf{k}) \rho^*(\mathbf{k}) \right] \\
&= \frac{1}{\lambda_B^{3N} N!} \exp \left[\frac{1}{2} N \beta U(0) \right] \prod_{\mathbf{k} \neq 0} \left(\frac{4}{\pi \beta \phi(\mathbf{k})} \right)^{\frac{1}{2}} \int \prod_{\mathbf{k} > 0} d\sigma(\mathbf{k}) \exp \left[-\frac{1}{2} \sum_{\mathbf{k}} \frac{\sigma^*(\mathbf{k}) \sigma(\mathbf{k})}{\beta \phi(\mathbf{k})} \right] \\
&\int d\mathbf{R}^N \exp \left[-i \sum_{\mathbf{k}} \sigma(\mathbf{k}) \rho^*(\mathbf{k}) \right],
\end{aligned} \tag{15}$$

where $\exp \left[\frac{1}{2} N \beta U(0) \right]$ is from the self-interaction term of the CG Hamiltonian. The last term in Eq. (15) involving an integral over configurations can be further simplified due to the particular form of $\rho^*(\mathbf{k})$ as

$$\begin{aligned}
\int d\mathbf{R}^N \exp \left(-i \sum_{\mathbf{k}} \sigma(\mathbf{k}) \rho^*(\mathbf{k}) \right) &= \int d\mathbf{R}^N \exp \left(-i \sum_{\mathbf{k}} \sigma(\mathbf{k}) \sum_I \exp(i\mathbf{k} \cdot \mathbf{R}_I) \right) \\
&= \int d\mathbf{R}^N \exp \left(-i \sum_I \sigma(\mathbf{R}_I) \right) = \left(\int d\mathbf{R} \exp(-i\sigma(\mathbf{R})) \right)^N.
\end{aligned} \tag{16}$$

Note that Eq. (16) contains some imaginary values in the exponential function, and in principle, this will give rise to the numerical phase problem in sampling this integral. We will now refer to this integral as a *phase integral* and later discuss how this phase problem is exacerbated in the case of grand canonical ensembles. From Eqs. (15) and (16), one can finally obtain an expression of the canonical partition function as a functional integral with respect to an auxiliary field

$$\mathcal{Z}(N, V, T) = \frac{1}{\lambda_B^{3N} N!} \int d\mu(\sigma(\mathbf{R})) \exp(-\mathcal{S}[\sigma(\mathbf{R})]), \tag{17}$$

in which the integral measure is defined as

$$d\mu[\sigma] = \exp \left(\frac{1}{2} N \beta \phi(0) \right) \exp \left[-\frac{\beta}{2} \phi(\mathbf{k} = 0) N^2 \right] \prod_{\mathbf{k} \neq 0} \left(\frac{4}{\pi \beta \phi(\mathbf{k})} \right)^{\frac{1}{2}} \prod_{\mathbf{k} > 0} d\sigma_R(\mathbf{k}) d\sigma_I(\mathbf{k}), \tag{18}$$

and the effective action functional $\mathcal{S}[\sigma(\mathbf{R})]$ takes the following form,

$$\mathcal{S}[\sigma(\mathbf{R})] = \frac{1}{2} \sum_{\mathbf{k} \neq 0} \frac{\sigma^*(\mathbf{k}) \sigma(\mathbf{k})}{\beta \phi(\mathbf{k})} - N \ln \int d\mathbf{R} e^{-i\sigma(\mathbf{R})}. \tag{19}$$

In turn, for positive Fourier modes, Eqs. (17)-(19) suggest that the HS transformation can be readily applied to derive the field-theoretical description of the CG Hamiltonian. This approach is numerically advantageous, as the computational overhead depends only on the number of k -points, n_k , rather than the number of particles N . Therefore, consistent with the efficacy of SCFT for polymeric systems, this method allows for efficiently describing the effective partition function at

the field-theoretical level for large-scale molecular systems exhibiting non-trivial correlations where $N \gg n_k$. Based on this formulation, an effective strategy for sampling structural estimators will be discussed in Paper II.¹³²

D. General Fourier Modes: Generalized Mode Theory

The findings of the previous Subsection C cannot be directly applied to the case of negative weights $a < 0$ in the $\exp\left(-\frac{1}{2}ax^2\right)$ form. Nevertheless, if $a < 0$, one can instead perform the HS transformation on $-a$, leading to the following relationship:

$$\exp\left(-\frac{1}{2}ax^2\right) = \frac{1}{\sqrt{2\pi|a|}} \int dy \exp\left(-\frac{y^2}{2|a|} + xy\right). \quad (20)$$

Equation (20) indicates that the negative Fourier modes of the pairwise interaction can also be transformed by the modified HS transformation. To generalize this approach for treating arbitrary Fourier modes that may include mixed positive and negative modes, our central claim is that one can decompose the real part of the Fourier modes of the pairwise interaction into two components $\phi(\mathbf{k}) = v(\mathbf{k}) + \omega(\mathbf{k})$, where $v(\mathbf{k})$ is always positive, while $\omega(\mathbf{k})$ remains negative for any reciprocal lattice vector \mathbf{k} . This decomposition is unique given the Fourier-transformed $\phi(\mathbf{k})$ modes. By performing this decomposition, the CG Hamiltonian in reciprocal space can be expressed as:

$$\begin{aligned} U(\mathbf{R}^N) &= \frac{1}{2} \sum_{\mathbf{k}} \rho^*(\mathbf{k}) U(\mathbf{k}) \rho(\mathbf{k}) - \frac{1}{2} NU(0) \\ &= \frac{1}{2} \sum_{\mathbf{k}} \rho^*(\mathbf{k}) (v(\mathbf{k}) + \omega(\mathbf{k})) \rho(\mathbf{k}) - \frac{1}{2} NU(0) \end{aligned} \quad (21)$$

Our generalized mode theory can transform arbitrary CG interactions into a field-theoretical model by introducing an auxiliary field variable. In the case of the positive mode component, $v(\mathbf{k})$, the HS transformation yields two auxiliary field variables $\sigma_R(\mathbf{k})$ and $\sigma_I(\mathbf{k})$ for $\mathbf{k} \neq 0$, as discussed in the previous section:

$$\begin{aligned} \exp\left[-\frac{1}{2}\beta \sum_{\mathbf{k} \neq 0} \rho^*(\mathbf{k}) v(\mathbf{k}) \rho(\mathbf{k})\right] &= \prod_{\mathbf{k} \neq 0} \left(\frac{4}{\pi\beta v(\mathbf{k})}\right)^{\frac{1}{2}} \int \prod_{\mathbf{k} > 0} d\sigma_R(\mathbf{k}) d\sigma_I(\mathbf{k}) \\ &\times \exp\left[-\frac{1}{2} \sum_{\mathbf{k} \neq 0} \frac{\sigma^*(\mathbf{k}) \sigma(\mathbf{k})}{\beta v(\mathbf{k})} - i \sum_{\mathbf{k} \neq 0} \sigma(\mathbf{k}) \rho^*(\mathbf{k})\right]. \end{aligned} \quad (22)$$

For the negative part, the modified HS transform [Eq. (20)] is applied to the second auxiliary field $\xi(\mathbf{k}) := \xi_R(\mathbf{k}) + i\xi_I(\mathbf{k})$, giving

$$\exp\left[-\frac{1}{2}\beta \sum_{\mathbf{k} \neq 0} \rho^*(\mathbf{k}) \omega(\mathbf{k}) \rho(\mathbf{k})\right] = \prod_{\mathbf{k} \neq 0} \left(\frac{4}{\pi\beta |\omega(\mathbf{k})|}\right)^{\frac{1}{2}} \int \prod_{\mathbf{k} > 0} d\xi_R(\mathbf{k}) d\xi_I(\mathbf{k})$$

$$\times \exp \left[-\frac{1}{2} \sum_{\mathbf{k} \neq 0} \frac{\xi^*(\mathbf{k})\xi(\mathbf{k})}{\beta|\omega(\mathbf{k})|} + \sum_{\mathbf{k} \neq 0} \xi(\mathbf{k})\rho^*(\mathbf{k}) \right]. \quad (23)$$

Similar to the positive mode case, the canonical partition function does not explicitly require the zero wave vector contribution of $\phi(\mathbf{k} = 0)$, but the underlying reasoning is slightly different. While the generalized Fourier mode decomposition implies that one should consider both $v(\mathbf{k})$ and $\xi(\mathbf{k})$, i.e., $\phi(\mathbf{k} = 0) = v(\mathbf{k} = 0) + \xi(\mathbf{k} = 0)$, at the zero wave vector, either $v(\mathbf{k} = 0)$ or $\xi(\mathbf{k} = 0)$ vanishes to zero due to its sign, i.e., $\exp(0) = 1$. Hence, it reduces to the case of the positive Fourier mode, and then the remaining factor becomes

$$\exp \left[-\frac{\beta}{2} (v(\mathbf{k} = 0) + \xi(\mathbf{k} = 0))N^2 \right] = \exp \left[-\frac{\beta}{2} \phi(\mathbf{k} = 0)N^2 \right]. \quad (24)$$

By combining Eqs. (22) and (23) with the zero wave vector contribution, we arrive at the bottom-up field-theoretical representation of the canonical partition function, expressed as:

$$\begin{aligned} \mathcal{Z}(N, V, T) &= \frac{1}{\lambda_B^{3N} N!} \exp \left(\frac{1}{2} \beta N U(0) \right) \exp \left[-\frac{\beta}{2} \phi(\mathbf{k} = 0)N^2 \right] \prod_{\mathbf{k} \neq 0} \left[\left(\frac{4}{\pi \beta v(\mathbf{k})} \right)^{\frac{1}{2}} \cdot \left(\frac{4}{\pi \beta |\omega(\mathbf{k})|} \right)^{\frac{1}{2}} \right] \\ &\times \int \mathcal{D}\sigma(\mathbf{R}) \mathcal{D}\xi(\mathbf{R}) \left\{ \exp \left[-\frac{1}{2} \sum_{\mathbf{k} \neq 0} \left(\frac{\sigma^*(\mathbf{k})\sigma(\mathbf{k})}{\beta v(\mathbf{k})} + \frac{\xi^*(\mathbf{k})\xi(\mathbf{k})}{\beta |\omega(\mathbf{k})|} \right) \right] \times \left(\int d\mathbf{R} \exp(-i\sigma(\mathbf{R}) + \xi(\mathbf{R})) \right)^N \right\}. \end{aligned} \quad (25)$$

In Eq. (25), the integrands are abbreviated as $\mathcal{D}\sigma(\mathbf{R}) := \prod_{\mathbf{k} > 0} d\sigma_R(\mathbf{k}) d\sigma_I(\mathbf{k})$ and $\mathcal{D}\xi(\mathbf{R}) := \prod_{\mathbf{k} > 0} d\xi_R(\mathbf{k}) d\xi_I(\mathbf{k})$. To reveal the mathematical structure more clearly, Eq. (25) can be compactly expressed as

$$\mathcal{Z}(N, V, T) = \frac{1}{\lambda_B^{3N} N!} \int d\mu(\sigma, \xi) \exp(-S[\sigma, \xi]), \quad (26)$$

where the integration measure is defined as

$$\begin{aligned} d\mu(\sigma, \xi) &:= \exp \left(\frac{1}{2} \beta N U(0) \right) \exp \left[-\frac{\beta}{2} \phi(\mathbf{k} = 0)N^2 \right] \prod_{\mathbf{k} \neq 0} \left[\left(\frac{4}{\pi \beta v(\mathbf{k})} \right)^{\frac{1}{2}} \right. \\ &\quad \left. \cdot \left(\frac{4}{\pi \beta |\omega(\mathbf{k})|} \right)^{\frac{1}{2}} \right] \mathcal{D}\sigma(\mathbf{R}) \mathcal{D}\xi(\mathbf{R}), \end{aligned} \quad (27)$$

and the action functional can be written as

$$S[\sigma, \xi] = \frac{1}{2} \sum_{\mathbf{k} \neq 0} \left[\frac{1}{\beta v(\mathbf{k})} \sigma^*(\mathbf{k})\sigma(\mathbf{k}) + \frac{1}{\beta |\omega(\mathbf{k})|} \xi^*(\mathbf{k})\xi(\mathbf{k}) \right] - N \ln \int d\mathbf{R} e^{-i\sigma(\mathbf{R}) + \xi(\mathbf{R})}. \quad (28)$$

It is worth noting that in the effective action functional defined in Eq. (28), the terms associated with the auxiliary field variable $\xi(\mathbf{R})$ in the phase integral are always real and correspond to

positive statistical weights. Therefore, they do not contribute to the numerical phase problem in Monte Carlo sampling. The primary numerical challenges arise from the positive Fourier modes.

IV. Field-theoretical Transformation: Grand Canonical Theory

In field-theoretical simulations, grand canonical systems, where the number of particles changes, are more desirable. This preference arises because brute-force atomistic simulations of such large chemical systems encounter computational and numerical limitations, e.g., particle insertion at high densities in traditional grand canonical Monte Carlo methods.⁹ Yet, the canonical description of the field-level partition function serves as a starting point for deriving the grand canonical-level description of classical field models. The general structure of extending the single-component case to a multi-component case remains invariant under the grand canonical ensembles (interaction profiles do not change). Therefore, in this section, we primarily discuss the single-component case for conciseness.

A. Positive Fourier Modes

The grand canonical partition function $\Theta(\mu, V, T)$ is derived based on the canonical partition function:

$$\Theta(\mu, V, T) = \sum_{N=0}^{\infty} e^{\beta\mu N} \mathcal{Z}(N, V, T). \quad (29)$$

The mathematical structure of $\Theta(\mu, V, T)$ at the field-level involves extracting the Gaussian measure outside of Σ_N and grouping $e^{\beta\mu N}$ with the self-energy term $\exp\left(\frac{1}{2}N\beta\phi(0)\right)$ and the phase integral, i.e., $\left(\int d\mathbf{R} \exp(-i\sigma(\mathbf{R}))\right)^N = \exp\left(N \ln \int d\mathbf{R} e^{-i\sigma(\mathbf{R})}\right)$. Importantly, for grand canonical systems, we can introduce the zero wave vector component of $\rho(\mathbf{k})$ (as the number of particles changes). In this case, the HS transformation of the zero mode becomes

$$\exp\left[-\frac{\beta}{2}\rho^*(\mathbf{k}=0)\phi(\mathbf{k}=0)\rho(\mathbf{k}=0)\right] = \frac{1}{\sqrt{2\pi\beta\phi(0)}} \int d\sigma(0) \dots = \frac{1}{2\sqrt{2}} \sqrt{\frac{4}{\pi\beta\phi(0)}} \int d\sigma(0) \dots, \quad (30)$$

This implies that the action functional and integration measure now spans all \mathbf{k} vectors, including $\mathbf{k} = 0$.

In order to separate out the N -dependence, we define an N -independent integral measure [which is now possible because we decoupled $\sigma(0)$], $d\tilde{\mu}[\sigma]$, as $d\mu[\sigma]d\sigma(0) = \exp\left(\frac{1}{2}N\beta\phi(0)\right)d\tilde{\mu}[\sigma]$, giving

$$\Theta(\mu, V, T) = \int d\tilde{\mu}[\sigma(\mathbf{R})] \exp\left(-\frac{1}{2} \sum_{\mathbf{k}} \frac{\sigma^*(\mathbf{k})\sigma(\mathbf{k})}{\beta\phi(\mathbf{k})}\right) \sum_{N=0}^{\infty} \frac{1}{\lambda_B^{3N} N!} \exp\left[N\left(\beta\mu + \frac{1}{2}\beta\phi(0) + \ln \int d\mathbf{R} e^{-i\sigma(\mathbf{R})}\right)\right]. \quad (31)$$

We can further simplify Eq. (31) as follows. First, as μ, λ_B , and $\phi(0)$ are constants or system-dependent coefficients, we can group them as a fugacity-like constant, χ , defined as $\chi :=$

$\exp\left(\beta\mu + \frac{1}{2}\beta\phi(0)\right)/\lambda_B^3$. Then, we then notice that a term inside $\Sigma_{N=0}^\infty$ is simply a Taylor expansion of $\exp(\chi \int d\mathbf{R} e^{-i\sigma(\mathbf{R})}) = \sum_N \frac{\chi^N}{N!} \left(\int d\mathbf{R} e^{-i\sigma(\mathbf{R})}\right)^N$.

Next is the integral measure $d\tilde{\mu}[\sigma]$. By incorporating the zero wave vector contribution, as noted in Eq. (30), we can simplify $\Theta(\mu, V, T)$ as

$$\begin{aligned}\Theta(\mu, V, T) &:= \int \mathcal{D}\mu[\sigma(\mathbf{R})] \exp\left(-\frac{1}{2} \sum_{\mathbf{k}} \frac{\sigma^*(\mathbf{k})\sigma(\mathbf{k})}{\beta\phi(\mathbf{k})}\right) \exp\left(\chi \int d\mathbf{R} e^{-i\sigma(\mathbf{R})}\right) \\ &:= \int \mathcal{D}\mu[\sigma(\mathbf{R})] \exp(-S_{\text{GC}}[\sigma(\mathbf{R})]),\end{aligned}\tag{32}$$

with $\mathcal{D}\mu[\sigma(\mathbf{R})] := \frac{1}{2\sqrt{2}} \prod_{\mathbf{k}} \sqrt{\frac{4}{\pi\beta\phi(\mathbf{k})}} d\sigma(0) \prod_{\mathbf{k}>0} d\sigma_R(\mathbf{k}) d\sigma_I(\mathbf{k})$. Note that the $1/2\sqrt{2}$ prefactor is due to $\mathbf{k} = 0$ contribution. Alternatively, one can decouple the $\phi(\mathbf{k})$ dependence from the integral measure $\mathcal{D}\mu[\sigma(\mathbf{R})]$ by introducing a normalization constant for $\phi(\mathbf{k})$ defined as $\gamma_\phi = \frac{1}{2\sqrt{2}} \prod_{\mathbf{k}} \sqrt{\frac{4}{\pi\beta\phi(\mathbf{k})}}$, giving

$$\mathcal{D}\mu[\sigma(\mathbf{R})] = \gamma_\phi d\sigma(0) \prod_{\mathbf{k}>0} d\sigma_R(\mathbf{k}) d\sigma_I(\mathbf{k}).\tag{33}$$

Note that the multiplication now involves all \mathbf{k} vectors (whereas $\mathbf{k} \neq 0$ for the canonical case), and the effective action functional in grand canonical ensembles can now be expressed as

$$S_{\text{GC}}[\sigma(R)] := \frac{1}{2} \sum_{\mathbf{k}} \frac{\sigma^*(\mathbf{k})\sigma(\mathbf{k})}{\beta\phi(\mathbf{k})} - \chi \int d\mathbf{R} e^{-i\sigma(\mathbf{R})}.\tag{34}$$

The major difference between the grand canonical action and the canonical action is that the imaginary part is in an exponential form. This suggests that the phase problem for sampling this integral will be significantly more challenging compared to the canonical case. Such numerical instability requires an effective numerical sampling method to further reduce statistical noise when sampling grand canonical field models. Details about the sampling algorithm will be presented in the following Sec. VII.

B. General Fourier Modes: Generalized Mode Theory

Now, we extend our findings from Sec. IV. A. to the case of general Fourier modes. The underlying idea remains the same as in the canonical case, where we separate the Fourier-transformed interaction $\phi(\mathbf{k})$ into two parts: the positive-definite $\nu(\mathbf{k})$ and the negative-definite $\omega(\mathbf{k})$. This allows us to express the grand canonical partition function as:

$$\Theta(\mu, V, T) = \sum_{N=0}^{\infty} e^{\beta\mu N} \mathcal{Z}(N, V, T) = \int \mathcal{D}\mu[\sigma, \xi] \exp(-S_{\text{GC}}[\sigma, \xi]).\tag{35}$$

The effective action functional with respect to the auxiliary fields σ and ξ is expressed as,

$$S_{GC}[\sigma, \xi] := \frac{1}{2} \sum_{\mathbf{k}} \left[\frac{1}{\beta v(\mathbf{k})} \sigma^*(\mathbf{k}) \sigma(\mathbf{k}) + \frac{1}{\beta |\omega(\mathbf{k})|} \xi^*(\mathbf{k}) \xi(\mathbf{k}) \right] - \chi \int d\mathbf{R} e^{-i\sigma(\mathbf{R}) + \xi(\mathbf{R})}, \quad (36)$$

and the integral measure $\mathcal{D}\mu[\sigma, \xi]$ includes the zero wave vector contributions from both $\sigma(\mathbf{R})$ and $\xi(\mathbf{R})$ and is defined as

$$\mathcal{D}\mu[\sigma, \xi] := \frac{1}{8} \prod_{\mathbf{k}} \left[\sqrt{\frac{4}{\pi \beta v(\mathbf{k})}} \cdot \sqrt{\frac{4}{\pi \beta |\omega(\mathbf{k})|}} \right] d\sigma(0) d\xi(0) \prod_{\mathbf{k} > 0} d\sigma_R(\mathbf{k}) d\sigma_I(\mathbf{k}) d\xi_R(\mathbf{k}) d\xi_I(\mathbf{k}). \quad (37)$$

Equations (35)-(37) are the main results of this subsection. Similar to Eqs. (26)-(28), we observe that $\omega(\mathbf{k})$ does not contribute to the phase problem, even though its magnitude increases exponentially. The primary challenge in implementing Eqs. (36) and (37) is to address the contribution from $\sigma(\mathbf{R})$ through $v(\mathbf{k})$.

V. Perturbative Treatment of Fourier Modes

A. Perturbative Treatment in Reciprocal Space

The findings from the previous sections demonstrated that introducing auxiliary fields can effectively reformulate partition functions in reciprocal space. While, in principle, $\phi(\mathbf{k}) = v(\mathbf{k}) + \omega(\mathbf{k})$ does not inherently suffer from numerical issues, the resulting profile for either $v(\mathbf{k})$ or $\omega(\mathbf{k})$ exhibits a discontinuous Fourier spectrum as it crosses zero. Since the HS transformation is applied separately to $v(\mathbf{k})$ and $\omega(\mathbf{k})$, this leads to two separate transformations being performed on spiky, discontinuous Fourier modes derived from molecular CG interactions. More importantly, the auxiliary fields $\sigma(\mathbf{k})$ and $\xi(\mathbf{k})$, which are sampled from these discontinuous Fourier profiles, may contribute to numerical issues, particularly when handling more complex systems such as multi-component systems with distinct interactions. Introducing additional particle types into a system increases the number of auxiliary fields to six (or ten in generalized modes), with even more field variables required for systems beyond two components. While a detailed discussion of multi-component systems will be provided in Paper II,¹³² it is important to develop computationally efficient methods for sampling Fourier profiles as an effective theory.

For the single-component system, a minimalist Fourier representation of the given CG system can be constructed by focusing solely on the short wave vector profile with positive (repulsive) values. In this approximation, we only need one auxiliary variable, $\sigma(\mathbf{k})$. This choice is inspired by the hard sphere description in classical perturbation theory of liquids, where short-range repulsive interactions in real space dominate the overall structural correlations.^{133, 134} Recent studies have also shown that this description can be faithfully extended to CG dynamics.¹³⁵⁻¹³⁹ Therefore, the main objective of the remainder of this section is to explore if classical perturbation treatments can help mitigate the numerical challenges associated with sampling auxiliary fields in reciprocal space. We will examine in particular the case of single-component systems (single interaction space) under different perturbations. This should, in principle, provide a systematic design principle for extending these ideas to multi-component systems, much like the classical perturbation theory of liquid mixtures in real space.

However, some differences should be noted for the reciprocal space representation in this context. First, the Fourier interaction profile $U(\mathbf{k})$ will be fairly different from the real-space interaction profile, as the short-range (real-valued) repulsive interaction is smeared across the entire k -space via the Fourier transform. While the intermediate particle-based coarse-graining process helps mitigate the challenges of sampling a diverging profile as $R \rightarrow 0$ at the atomistic level (where the Fourier transformation is ill-defined), this approach results in non-continuous CG potentials in the radial domain. In such cases, one can employ *ad hoc* approximations, such as introducing a finite cutoff value^{140, 141} to account for the missing short-range interactions or extrapolating these regime using hard-core repulsions based on Ref. 31, followed by perturbation theory in reciprocal space.¹⁴² However, the systematic determination of $U(\mathbf{k})$ is not the main focus of this paper. Instead, this section presents our perspective using an analytical, continuous CG interaction as an illustrative example, given by

$$U^{\text{ref}}(R) = 15 \frac{\sin\left(\frac{R}{1.25}\right)}{R} \left[\frac{1}{2} \left(1 - \tanh\left(\frac{R - 1.25\pi}{0.8}\right) \right) \right], \quad (38)$$

where R is in Å units. Equation (38) possesses several advantageous characteristics for investigating our approach. In real space, $U^{\text{ref}}(R)$ exhibits both short-range repulsion and long-range attraction. Importantly, the strength of the long-range interaction is smaller than that of the repulsion, which results in a stable structural profile. This interaction potential satisfies $\hat{U}^{\text{ref}}(\mathbf{k} = 0) = \int_0^\infty d\mathbf{R} U^{\text{ref}}(\mathbf{R}) e^{-i(\mathbf{k}=0) \cdot \mathbf{R}} > 0$ in Fourier space, as shown in Fig. 2(a), where we can approximate it with a positive Fourier mode.

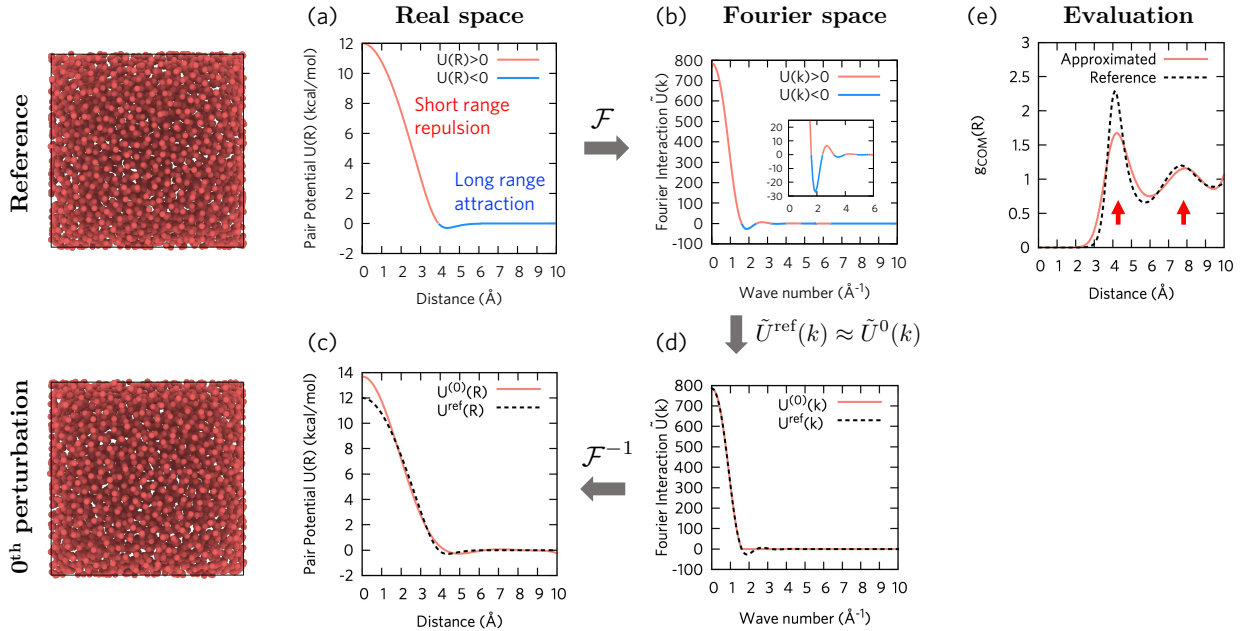


Figure 2: Perturbation treatment of Fourier modes: zeroth-order approximation. (a)-(b): Reference model using $U^{\text{ref}}(R)$ [Eq. (38)] and (c)-(d): zeroth-order perturbation using the short-range repulsion $\hat{U}^{(0)}(\mathbf{k})$. From $U^{\text{ref}}(R)$ [panel (a)], the reference Fourier mode was obtained using $\hat{U}^{\text{ref}} = \mathcal{F}[U^{\text{ref}}(R)]$ [panel (b)], and then the short-range wavevector was chosen as $\hat{U}^{(0)}(\mathbf{k})$ [panel (d)]. Finally, the real-space representation $U^{(0)}(R)$ was obtained using $U^{(0)} = \mathcal{F}^{-1}[\hat{U}^{(0)}(\mathbf{k})]$ [panel (c)]. The performance of the zeroth-order approximation was evaluated by performing the

particle-level simulation and computing the radial distribution function [panel (e)], where the general coordination structure was correctly captured (red arrows). The snapshot for each model during particle-level simulation was depicted on the left side to show the similarity compared to the reference.

While our model exhibits a finite repulsion value at $R = 0$, this value was set to $20k_B T$ by design to avoid any significant sampling at this distance, see Appendix B for computational details. As illustrated in Fig. 2(e), our model is non-penetrable, distinguishing it from the Gaussian Core Model, which often shows penetration behavior of molecules at the zero distance in liquids, i.e., $g(R = 0) > 0$. Therefore, our choice of CG interaction can be considered as a realistic representation of truncated hard-core CG interactions, containing both repulsion and attraction in real space.

B. Zeroth-order Approximation

Before attempting the perturbative approximation, we numerically estimated the Fourier transform of $U^{\text{ref}}(\mathbf{R})$ using $\hat{U}^{\text{ref}}(\mathbf{k}) = \int_0^\infty d\mathbf{R} U^{\text{ref}}(\mathbf{R}) e^{-i\mathbf{k}\cdot\mathbf{R}}$. Even though the real-space interaction features only one repulsive region and one attractive region, we observed that reciprocal space in Fig. 2(b) is divided by several regions where $\phi(\mathbf{k}) > 0$ or $\phi(\mathbf{k}) < 0$. The long wave vector region exhibits an oscillatory profile that continuously transitions between negative and positive Fourier modes. This behavior is expected due to the nature of Fourier transformation and confirms our argument that a naïve decomposition approach might lead to highly discontinuous $v(\mathbf{k})$ and $\omega(\mathbf{k})$, contributing to numerical instability. Despite the oscillatory profile, we note that the primary contribution to the Fourier-transformed interaction comes from the short wave vector repulsion, with the strongest attraction being only about 4% of the magnitude in Fig. 2(b). This relative difference suggests that we can approximate the overall Fourier-transformed profile by primarily considering the short-range repulsion profile (in \mathbf{k} space), akin to the perturbation treatment: $\hat{U}^{\text{ref}}(\mathbf{k}) \approx \hat{U}^{(0)}(\mathbf{k})$ [Fig. 2(d)]. This approximation resembles the hard sphere approximation in real space,¹⁴³ and is hereafter referred to as the zeroth-order approximation.

The fidelity of the zeroth-order perturbation can be indirectly confirmed by evaluating the inverse Fourier transformation of $\hat{U}^{(0)}(\mathbf{k})$, i.e., $U^{(0)}(\mathbf{R}) = \int_0^\infty d\mathbf{k} \hat{U}^{(0)}(\mathbf{k}) e^{i\mathbf{k}\cdot\mathbf{R}}$ then performing particle-level MD simulations using $U^{(0)}(\mathbf{R})$. While this indirect examination does not involve any field-theoretical simulations, it provides a general principle of how $\hat{U}^{(0)}(\mathbf{k})$ should behave under sufficient field sampling, without the burden of additional approximations and numerical settings associated with field-level simulations. From the inverse Fourier transformed profile, we can see that neglecting higher-order wave vector contributions mainly lowers the $U^{(0)}(\mathbf{R} = 0)$ value, as shown in Fig. 2(c). Since this region is infinitesimally sampled during the MD simulation, this profile suggests that the zeroth-order perturbation does not significantly change the interaction profile, although some changes in the attractive well are noted [since $\hat{U}^{(0)}(\mathbf{k})$ still affects entire pair distance space]. From the MD simulation of the approximated Fourier profile, this slight change in the attractive well results in a less structured profile, as seen from the RDF [Fig. 2(e)]. However, this approximation still correctly reproduces the pair distances of the first and second coordination shells (red arrows). Additionally, the similarity in the MD snapshots depicted in Fig. 2 indicates that the zeroth-order perturbation offers dynamics close to the atomistic reference. In turn, our analysis suggests that the zeroth-order approximation in reciprocal space can be utilized as an efficient approximation to sample the highly oscillatory field with relatively low

computational cost, as it involves only a single auxiliary field variable. Nevertheless, the agreement is not as pronounced as the zeroth-order approximation in real space (hard sphere) because the hard sphere interaction is smeared into the whole \mathbf{k} space through Fourier transformation.

C. First-order Approximation

Following a similar hierarchical approach to that seen in classical perturbation theory^{133, 134} or analytical models, such as the generalized van der Waals theory,^{144, 145} the next step would be to incorporate the next strongest attraction in reciprocal space, which we referred to as the first-order approximation. In our example, as depicted in Fig. 3(a), the first-order approximation includes a non-zero $\tilde{U}^{(1)}(\mathbf{k})$ value up to $k = 2.5 \text{ \AA}^{-1}$. This necessitates the introduction of the second field variable while minimizing numerical instability by ignoring contributions from $k > 2.5 \text{ \AA}^{-1}$. However, as observed in the zeroth-order approximation, this perturbative representation in reciprocal space does not directly correspond to the real-space interaction.

We then evaluate the performance of the first-order approximation by conducting the particle-level MD simulations, following a procedure similar to that of the zeroth-order approximation, using the real-space interaction derived from the inverse Fourier transformation of the first-order approximation in \mathbf{k} space. Interestingly, contrary to our expectations, we observe significant differences between the first-order approximation and the reference interaction. The resulting structural correlations are notably distinct due to a strong long-range attraction (approximately -1 kcal/mol) in the first-order approximation, leading to unusually high correlations at long distances, as shown in Fig. 3(c). While the particle-level RDF initially appears to agree with the reference RDF within 8 \AA , it abruptly spikes to 10 at 10 \AA , an entirely unphysical behavior. In the MD trajectories depicted in Fig. 3, the particle dynamics resembles the atomistic snapshot (Fig. 2), but in terms of dynamics, the particles exhibit limited translational motion, similar to crystallization. This locking behavior can be attributed to the balance between a strong long-range attraction and short-range repulsion, but it no longer conforms to the reference dynamics.

This discrepancy is clearly opposite from the performance when including the perturbative attraction in conventional perturbation theory and also disproves the fidelity of perturbation theory in reciprocal space. Then, how should we understand this unusual behavior and design efficient Fourier modes of molecular CG interaction? In simple liquids, pair interaction profiles in real space generally exhibit short-range repulsions with relatively weaker long-range interactions. As the pair distance increases, this interaction decays to zero, since simple liquids do not exhibit long-range ordering. Therefore, it is reasonable to deconvolute the pair CG interaction $U_2(R)$ into a convolution of two radial functions

$$U_2(R) = \sigma(R) * \tilde{U}(R), \quad (39)$$

where $\sigma(R)$ is a sigmoid-like function that encodes the radially decaying feature of $U_2(R)$, and $\tilde{U}(R)$ represents a deconvoluted $U_2(R)$ using the $\sigma(R)$ filter. For simplicity, $\sigma(R)$ can be approximated as a square step function that decays from 1 to 0 after some cutoff distance R_{cut} , which is related to the characteristic length scale of liquids:

$$\sigma(R) = \begin{cases} 1 & (\text{if } R < R_{\text{cut}}) \\ 0 & (\text{otherwise}) \end{cases}.$$

(40)

Since the Fourier transform of the square-like step function is the sinc function, $\text{sinc}(x) = \sin(x)/x$, this deconvolution directly reveals that the radially decaying nature of CG interactions in simple liquids (as well as other molecular systems) inevitably introduces highly oscillating Fourier modes in reciprocal space. Since the sinc function constantly changes its sign over a period of wave vectors, Eq. (40) indicates that the large difference observed in the long-range regime for the first-order approximation in Fig. 3(b) is due to the lack of capturing these oscillatory Fourier modes.

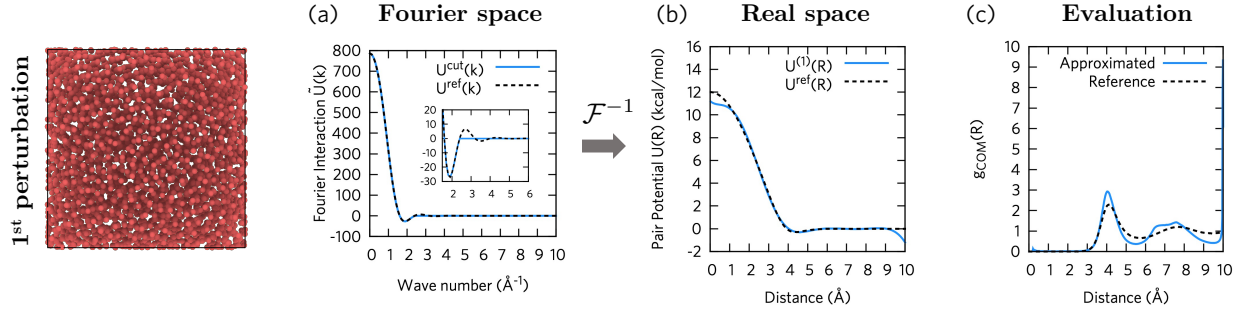


Figure 3: First-order perturbative approximation of the Fourier modes to the reference interaction (dotted black lines) from Figs. 2(a)-(b), where blue lines contain the short-range repulsion $\hat{U}^{(0)}(\mathbf{k})$ and the perturbative attraction in \mathbf{k} space. From the perturbed interaction in \mathbf{k} space [panel (a)], the real-space interaction $U^{(1)}(R)$ was obtained using $U^{(1)} = \mathcal{F}^{-1}[\hat{U}^{(1)}(\mathbf{k})]$ [panel (c)]. The performance of the approximation was evaluated by performing the particle-level simulation and computing the radial distribution function in panel (c) for $U^{(1)}$, in comparison with the reference structural correlations (dotted black lines).

VI. Conclusions and Outlook

In this work, we introduced a bottom-up strategy to systematically construct a statistical field theory for molecular liquids. Recognizing that scaling directly from microscopic (atomistic) statistics to a mesoscopic field-level description is practically infeasible (especially due to the “hard” short-ranged interactions), we devised a hierarchical coarse-graining (CG) method that incorporates a molecular CG-level model as an intermediate step in transforming the atomistic Hamiltonian to a field-theoretical representation. By reducing the number and complexity of interactions and softening intermolecular forces at the CG level, this approach simplifies the atomistic-to-field-theoretic transformation while preserving important microscopic structural correlations of the underlying fluid. The subsequent transformation from molecular CG models with pairwise interactions to a field-theoretical representation becomes more straightforward due to the harmonic structure of the CG Hamiltonian in terms of density operators in Fourier space. Unlike previous efforts, which often relied on top-down approaches for polymeric systems or employing simplified analytical interactions that can fail to accurately represent microscopic molecular physics, our hierarchical approach can at least in part eliminate *ad hoc* assumptions commonly found in field-theoretical models of molecular systems. Therefore, the main objective of this work was to significantly broaden the applicability and scope of field-theoretical coarse-graining by extending this methodology to arbitrary atomistic systems under various ensemble conditions.

Introducing the intermediate CG model helps reduce the number of degrees of freedom and, more importantly, transforms divergent atomistic force fields into finite CG interactions sampled through atomistic statistics. However, deriving a general expression that encompasses various types of CG interactions remains highly challenging, as many-body CG interactions can exhibit both positive and negative Fourier modes. In particular, the presence of negative Fourier modes poses challenges for employing the Hubbard-Stratonovich (HS) transformation. To address this, we developed a generalized mode theory that decomposes positive and negative Fourier modes, applying the HS transformation and its variants separately. By introducing four auxiliary field variables (two for each mode), we generalized this approach for both canonical and grand canonical ensembles at the CG level.

Nevertheless, a downside of this generalized mode theory is the doubling of auxiliary fields, which can lead to numerical instability and reduced efficiency for complex systems. Inspired by classical perturbation theory, we devised a perturbative decomposition of the complex Fourier modes. While formulating such a perturbative approach in reciprocal space is less straightforward than in real space, we demonstrated its utility by effectively reducing the fluctuating amplitude of Fourier modes into a single short wavelength mode. Although this zeroth-order perturbative treatment diminishes some structural characteristics arising from long wavelength contributions, it reasonably captures the structural ordering of the underlying liquid while reducing computational cost by a factor of two. This approach is expected to facilitate the design of effective field-theoretical models for multi-component systems, which will be explored in the companion paper.

It is worth noting that, aside from the *ad hoc* approaches mentioned earlier, there are methods for simulating molecular liquids using field theory in limited cases based on the reaction interaction site model (RISM).^{67, 69, 70} In three-dimensional (3D) RISM,¹⁴⁶⁻¹⁴⁹ a field description of structures and interactions exerted by solvents can be constructed by extending the Ornstein-Zernike integral equation.¹⁵⁰ For polymeric systems, Schweizer and Curro extended the RISM framework to the Polymer RISM (PRISM) framework,^{151, 152} which is suitable for liquid-like polymers. Despite successful applications of 3D RISM¹⁵³ and PRISM¹⁵⁴ theories, these methods have certain critical limitations.¹⁵⁵ These limitations mainly arise from their sensitivity to the choice of closures, approximations, and numerical solvers (e.g., Picard or inexact Newton), restricting their application to complex molecular systems with not liquid-like structural correlations. In order to demonstrate the fidelity of our CG framework compared to these existing approaches, it is essential to develop both a numerical framework and methods for sampling structural correlations at the field-theoretical level. While our method is designed to yield a field-theoretical representation of molecular fluids with fewer approximations to the system Hamiltonian, the present work mainly aims to propose a theoretical model through hierarchical coarse-graining. Therefore, the companion paper will focus on developing sampling techniques and estimators for numerical implementation. Although sampling the auxiliary field partition function has historically been challenging in many-body physics,¹²⁹⁻¹³¹ we anticipate that, at the classical level, our approach will be easier to implement quantitatively using numerical techniques compared to Auxiliary Field Quantum Monte Carlo methods. In conclusion, this hierarchical coarse-graining framework establishes a bottom-up foundation for advancing field-theoretical modeling of molecular systems, enabling scalable and versatile multiscale simulations at larger length scales.

ACKNOWLEDGMENTS

This material is based upon work was supported by the National Science Foundation (NSF Grant CHE-2102677). Simulations were performed using computing resources provided by the University of Chicago Research Computing Center (RCC). J.J. gratefully acknowledges Dr. Ankit Mahajan and Professor David R. Reichman for insightful discussion and feedback. J.J. also thanks the Harper Dissertation Fellowship from the University of Chicago during his graduate studies and an Arnold O. Beckman Postdoctoral Fellowship (<http://dx.doi.org/10.13039/100000997>) during his postdoctoral appointment.

DATA AVAILABILITY

The data that support the findings of this work are available from the corresponding author upon request.

APPENDIX

A. Treatment of Bonded Interactions in Multiple-Site CG Models

In this Appendix, we demonstrate how intramolecular (bonded) interactions remain decoupled from the HS transformation. To effectively illustrate our perspective, we showcase bonded interactions for two-site models and three-site CG models with bond and angle potentials. The reasoning provided can be faithfully extended to longer chains or more complex intramolecular topologies.

1. Bonded interactions

Consider a two-site CG model where each molecule (total N) comprises two sites labeled \mathbf{R}_{2I} and \mathbf{R}_{2I+1} for the I -th molecule. We assume that the bonded potential between these CG sites follows a simple harmonic form:

$$U_{\text{bond}} = \sum_{I=1}^N \frac{k_b}{2} |\mathbf{R}_{2I} - \mathbf{R}_{2I+1}|^2, \quad (\text{A1})$$

where k_b is the bond constant. To see how bonded terms can be analytically integrate out, consider a single bond

$$u_{\text{bond}} = \frac{k_b}{2} |\mathbf{R}_2 - \mathbf{R}_1|^2. \quad (\text{A2})$$

The bond configuration integral over \mathbf{R}_1 and \mathbf{R}_2 is then

$$\mathcal{Z}_{\text{bond}}^{1-2} = \int d\mathbf{R}_1 d\mathbf{R}_2 \exp\left(-\frac{\beta k_b}{2} |\mathbf{R}_2 - \mathbf{R}_1|^2\right), \quad (\text{A3})$$

where $\beta = (k_B T)^{-1}$. By performing a change of variables from the canonical transformation $\bar{\mathbf{R}} := (\mathbf{R}_2 + \mathbf{R}_1)/2$ and $u := \mathbf{R}_2 - \mathbf{R}_1$, the integral over $\bar{\mathbf{R}}$ gives a factor of the total volume V , whereas the integral over u yields $[2\pi/(\beta k_b)]^{3/2}$. Combined these, we arrive at $\mathcal{Z}_{\text{bond}}^{1-2} = V[2\pi/(\beta k_b)]^{3/2}$, and the total bond configuration integral is

$$\mathcal{Z}_{\text{bond}} = V^N \left(\frac{2\pi}{\beta k_b} \right)^{\frac{3N}{2}}, \quad (\text{A4})$$

which contributes as a Gaussian factor to the overall partition function, independent of the HS decoupling step.

2. Angle interaction

For three-site CG molecules, the same logic extends to both bond lengths and angles. Suppose that each of the N molecules has sites \mathbf{R}_{3I} , \mathbf{R}_{3I+1} , and \mathbf{R}_{3I+2} . The intramolecular interactions for this three-site system can be expressed as:

$$U_{\text{intra}} = \sum_{I=1}^N \left[\frac{k_b}{2} |\mathbf{R}_{3I+1} - \mathbf{R}_{3I}|^2 + \frac{k_b}{2} |\mathbf{R}_{3I+2} - \mathbf{R}_{3I+1}|^2 + \frac{k_\theta}{2} |\theta_I - \theta_0|^2 \right], \quad (\text{A5})$$

where θ_I is the angle formed by the two bonds in the i -th molecule with the energy minimum angle θ_0 , and k_θ is an angle constant. Although the integral in Eq. (A5) is more complex than Eq. (A1) due to angular term, the analytical integral follows a similar structure. By transforming to appropriate internal coordinates [e.g., bond-angle-torsion (BAT) coordinates¹⁵⁶⁻¹⁵⁹] to handle bond lengths and angles, Eq. (A5) remains a Gaussian-like integral in bond distances, multiplied by an angular term. Importantly, none of the bond or angle terms in Eq. (A5) follow the density-density interaction form $\rho(\mathbf{k})\rho(\mathbf{k}')$ required by the HS transformation. Therefore, the HS transformation applied to non-bonded interactions for three-site molecules does not affect these intramolecular constraints.

In summary, for an arbitrary number of internal constraints (bonds, angles, dihedrals, etc.), these bonded interactions remain in the direct coordinate integral and do not require HS transformation. Consequently, for complex CG models involving many CG sites with non-bonded and bonded interactions, the resulting partition function naturally separates into an analytical integral over intramolecular coordinates and the HS-transformed portion of the free energy, capturing intermolecular interactions in a field representation. This separation ensures that multi-site CG liquids and complex molecular topologies can be incorporated into our framework without any loss of generality.

B. Computational Details

1. Carbon tetrachloride (CCl₄) simulation

The atomistic and CG models for liquid carbon tetrachloride were constructed based on our previous work.¹⁶⁰ The initial structure, comprising 1000 CCl₄ molecules, was arranged in a cubic box with a length of 50 Å. The Packmol program package¹⁶¹ was used to randomize the initial configuration, followed by energy minimization to remove artificial stresses introduced during system preparation. To equilibrate the system, constant NPT simulations were performed at 300 K and 1 atm for 1 ns. From the equilibrated configuration, the box size was fixed at 57.23 Å, and constant NVT simulations were conducted at 300 K for 5 ns using the Nosé-Hoover thermostat.^{162,}

¹⁶³ All MD simulations were carried out with the Large-scale Atomic/Molecular Massively Parallel Simulator (LAMMPS) program package.¹⁶⁴⁻¹⁶⁶

From the sampled *NVT* trajectory, we coarse-grained each CCl_4 molecule to its center-of-mass representation. At this reduced resolution, the effective CG interaction was determined using the force-matching technique, implemented in the OpenMSCG program suite.¹⁶⁷ Sixth-order B-spline functions with a resolution of 0.2 Å were employed to obtain the final interaction profiles.

2. Perturbative treatment simulation

In order to examine the perturbative treatment of $U^{\text{ref}}(R)$ in practice, we initially constructed a model system consisting of 4000 particles within a cubic box under periodic boundary conditions (real space). The reduced number density N/V was set to 0.01634, corresponding to a cubic box length of 62.556 Å. The initial configuration was prepared following the same protocol outlined in Appendix B 1. Constant *NVT* simulations were then conducted at 300 K for 0.5 ns to maintain the same density, using the same thermostat setting described in Appendix B 1.

REFERENCES

1. A. D. MacKerell Jr, D. Bashford, M. Bellott, R. L. Dunbrack Jr, J. D. Evanseck, M. J. Field, S. Fischer, J. Gao, H. Guo and S. Ha, "All-atom empirical potential for molecular modeling and dynamics studies of proteins," *J. Phys. Chem. B* **102** (18), 3586-3616 (1998).
2. D. Frenkel and B. Smit, *Understanding molecular simulation: from algorithms to applications*. (Elsevier, 2001).
3. M. Karplus and J. A. McCammon, "Molecular dynamics simulations of biomolecules," *Nat. Struct. Biol.* **9** (9), 646-652 (2002).
4. S. A. Adcock and J. A. McCammon, "Molecular dynamics: survey of methods for simulating the activity of proteins," *Chem. Rev.* **106** (5), 1589-1615 (2006).
5. G. A. Voth, *Coarse-graining of condensed phase and biomolecular systems*. (CRC press, 2008).
6. D. E. Shaw, P. Maragakis, K. Lindorff-Larsen, S. Piana, R. O. Dror, M. P. Eastwood, J. A. Bank, J. M. Jumper, J. K. Salmon and Y. Shan, "Atomic-level characterization of the structural dynamics of proteins," *Science* **330** (6002), 341-346 (2010).
7. T. Schlick, R. Collepardo-Guevara, L. A. Halvorsen, S. Jung and X. Xiao, "Biomolecular modeling and simulation: a field coming of age," *Q. Rev. Biophys.* **44** (2), 191-228 (2011).
8. M. G. Saunders and G. A. Voth, "Coarse-graining methods for computational biology," *Annu. Rev. Biophys.* **42**, 73-93 (2013).
9. M. P. Allen and D. J. Tildesley, *Computer simulation of liquids*. (Oxford university press, 2017).
10. A. J. Pak and G. A. Voth, "Advances in coarse-grained modeling of macromolecular complexes," *Curr. Opin. Struct. Biol.* **52**, 119-126 (2018).
11. F. Müller-Plathe, "Coarse-graining in polymer simulation: from the atomistic to the mesoscopic scale and back," *ChemPhysChem* **3** (9), 754-769 (2002).
12. H. A. Scheraga, M. Khalili and A. Liwo, "Protein-folding dynamics: overview of molecular simulation techniques," *Annu. Rev. Phys. Chem.* **58**, 57-83 (2007).
13. C. Peter and K. Kremer, "Multiscale simulation of soft matter systems—from the atomistic to the coarse-grained level and back," *Soft Matter* **5** (22), 4357-4366 (2009).
14. T. Murtola, A. Bunker, I. Vattulainen, M. Deserno and M. Karttunen, "Multiscale modeling of emergent materials: biological and soft matter," *Phys. Chem. Chem. Phys.* **11** (12), 1869-1892 (2009).

15. S. Riniker and W. F. van Gunsteren, "A simple, efficient polarizable coarse-grained water model for molecular dynamics simulations," *J. Chem. Phys.* **134** (8), 084110 (2011).
16. W. G. Noid, "Perspective: Coarse-grained models for biomolecular systems," *J. Chem. Phys.* **139** (9), 090901 (2013).
17. J. Jin, A. J. Pak, A. E. Durumeric, T. D. Loose and G. A. Voth, "Bottom-up Coarse-Graining: Principles and Perspectives," *J. Chem. Theory Comput.* **18** (10), 5759-5791 (2022).
18. W. G. Noid, "Perspective: Advances, challenges, and insight for predictive coarse-grained models," *J. Phys. Chem. B* **127** (19), 4174-4207 (2023).
19. S. Izvekov and G. A. Voth, "A multiscale coarse-graining method for biomolecular systems," *J. Phys. Chem. B* **109** (7), 2469-2473 (2005).
20. S. Izvekov and G. A. Voth, "Multiscale coarse graining of liquid-state systems," *J. Chem. Phys.* **123** (13), 134105 (2005).
21. W. G. Noid, J.-W. Chu, G. S. Ayton, V. Krishna, S. Izvekov, G. A. Voth, A. Das and H. C. Andersen, "The multiscale coarse-graining method. I. A rigorous bridge between atomistic and coarse-grained models," *J. Chem. Phys.* **128** (24), 244114 (2008).
22. W. G. Noid, P. Liu, Y. Wang, J.-W. Chu, G. S. Ayton, S. Izvekov, H. C. Andersen and G. A. Voth, "The multiscale coarse-graining method. II. Numerical implementation for coarse-grained molecular models," *J. Chem. Phys.* **128** (24), 244115 (2008).
23. Z. Cao and G. A. Voth, "The multiscale coarse-graining method. XI. Accurate interactions based on the centers of charge of coarse-grained sites," *J. Chem. Phys.* **143** (24), 243116 (2015).
24. J. Jin, Y. Han and G. A. Voth, "Coarse-graining involving virtual sites: Centers of symmetry coarse-graining," *J. Chem. Phys.* **150** (15), 154103 (2019).
25. R. McGreevy and L. Pusztai, "Reverse Monte Carlo simulation: a new technique for the determination of disordered structures," *Mol. Simul.* **1** (6), 359-367 (1988).
26. A. P. Lyubartsev and A. Laaksonen, "Calculation of effective interaction potentials from radial distribution functions: A reverse Monte Carlo approach," *Phys. Rev. E* **52** (4), 3730 (1995).
27. D. Reith, M. Pütz and F. Müller-Plathe, "Deriving effective mesoscale potentials from atomistic simulations," *J. Comput. Chem.* **24** (13), 1624-1636 (2003).
28. M. S. Shell, "The relative entropy is fundamental to multiscale and inverse thermodynamic problems," *J. Chem. Phys.* **129** (14), 144108 (2008).
29. A. Chaimovich and M. S. Shell, "Relative entropy as a universal metric for multiscale errors," *Phys. Rev. E* **81** (6), 060104 (2010).
30. A. Chaimovich and M. S. Shell, "Coarse-graining errors and numerical optimization using a relative entropy framework," *J. Chem. Phys.* **134** (9), 094112 (2011).
31. L. Lu, S. Izvekov, A. Das, H. C. Andersen and G. A. Voth, "Efficient, regularized, and scalable algorithms for multiscale coarse-graining," *J. Chem. Theory Comput.* **6** (3), 954-965 (2010).
32. J. F. Dama, A. V. Sinitskiy, M. McCullagh, J. Weare, B. Roux, A. R. Dinner and G. A. Voth, "The theory of Ultra-Coarse-Graining. 1. General principles," *J. Chem. Theory Comput.* **9** (5), 2466-2480 (2013).
33. A. Davtyan, J. F. Dama, A. V. Sinitskiy and G. A. Voth, "The theory of Ultra-Coarse-Graining. 2. Numerical implementation," *J. Chem. Theory Comput.* **10** (12), 5265-5275 (2014).

34. J. F. Dama, J. Jin and G. A. Voth, "The theory of Ultra-Coarse-Graining. 3. Coarse-grained sites with rapid local equilibrium of internal states," *J. Chem. Theory Comput.* **13** (3), 1010-1022 (2017).
35. J. F. Dama, J. Jin and G. A. Voth, "Correction to the theory of Ultra-Coarse-Graining. 3. Coarse-grained sites with rapid local equilibrium of internal states," *J. Chem. Theory Comput.* **14** (4), 2288-2288 (2018).
36. J. Jin, Y. Han and G. A. Voth, "Ultra-Coarse-Grained Liquid State Models with Implicit Hydrogen Bonding," *J. Chem. Theory Comput.* **14** (12), 6159-6174 (2018).
37. J. Jin and G. A. Voth, "Statistical Mechanical Design Principles for Coarse-Grained Interactions across Different Conformational Free Energy Surfaces," *J. Phys. Chem. Lett.* **14** (6), 1354-1362 (2023).
38. J. M. Grime and G. A. Voth, "Early stages of the HIV-1 capsid protein lattice formation," *Biophys. J.* **103** (8), 1774-1783 (2012).
39. J. M. Grime, J. F. Dama, B. K. Ganer-Pornillos, C. L. Woodward, G. J. Jensen, M. Yeager and G. A. Voth, "Coarse-grained simulation reveals key features of HIV-1 capsid self-assembly," *Nat. Commun.* **7** (1), 1-11 (2016).
40. A. J. Pak, J. M. Grime, P. Sengupta, A. K. Chen, A. E. Durumeric, A. Srivastava, M. Yeager, J. A. Briggs, J. Lippincott-Schwartz and G. A. Voth, "Immature HIV-1 lattice assembly dynamics are regulated by scaffolding from nucleic acid and the plasma membrane," *Proc. Natl. Acad. Sci. U.S.A.* **114** (47), E10056-E10065 (2017).
41. A. J. Pak, J. M. Grime, A. Yu and G. A. Voth, "Off-pathway assembly: A broad-spectrum mechanism of action for drugs that undermine controlled hiv-1 viral capsid formation," *J. Am. Chem. Soc.* **141** (26), 10214-10224 (2019).
42. A. Yu, K. A. Skorupka, A. J. Pak, B. K. Ganer-Pornillos, O. Pornillos and G. A. Voth, "TRIM5 α self-assembly and compartmentalization of the HIV-1 viral capsid," *Nat. Commun.* **11** (1), 1-10 (2020).
43. M. Gupta, A. J. Pak and G. A. Voth, "Critical mechanistic features of HIV-1 viral capsid assembly," *Sci. Adv.* **9** (1), eadd7434 (2023).
44. A. V. Sinitskiy and G. A. Voth, "Quantum mechanics/coarse-grained molecular mechanics (QM/CG-MM)," *J. Chem. Phys.* **148** (1), 014102 (2018).
45. A. V. Mironenko and G. A. Voth, "Density functional theory-based quantum mechanics/coarse-grained molecular mechanics: Theory and implementation," *J. Chem. Theory Comput.* **16** (10), 6329-6342 (2020).
46. D. Teng, A. V. Mironenko and G. A. Voth, "QM/CG-MM: Systematic Embedding of Quantum Mechanical Systems in a Coarse-Grained Environment with Accurate Electrostatics," *The Journal of Physical Chemistry A* **128** (29), 6061-6071 (2024).
47. P. Español, M. Serrano and I. Zuñiga, "Coarse-graining of a fluid and its relation with dissipative particle dynamics and smoothed particle dynamic," *Int. J. Mod. Phys. C* **8** (04), 899-908 (1997).
48. P. Espanol and P. B. Warren, "Perspective: Dissipative particle dynamics," *J. Chem. Phys.* **146** (15) (2017).
49. E. G. Flekkøy and P. V. Coveney, "From molecular dynamics to dissipative particle dynamics," *Phys. Rev. Lett.* **83** (9), 1775 (1999).
50. E. G. Flekkøy, P. V. Coveney and G. De Fabritiis, "Foundations of dissipative particle dynamics," *Phys. Rev. E* **62** (2), 2140 (2000).

51. A. Eriksson, M. N. Jacobi, J. Nyström and K. Tunström, "On the microscopic foundation of dissipative particle dynamics," *Europhys. Lett.* **86** (4), 44001 (2009).
52. K. R. Hadley and C. McCabe, "On the investigation of coarse-grained models for water: balancing computational efficiency and the retention of structural properties," *J. Phys. Chem. B* **114** (13), 4590-4599 (2010).
53. S. Izvekov and B. M. Rice, "Multi-scale coarse-graining of non-conservative interactions in molecular liquids," *J. Chem. Phys.* **140** (10) (2014).
54. J. Zavadlav, S. J. Marrink and M. Praprotnik, "Adaptive resolution simulation of supramolecular water: the concurrent making, breaking, and remaking of water bundles," *J. Chem. Theory Comput.* **12** (8), 4138-4145 (2016).
55. J. Zavadlav and M. Praprotnik, "Adaptive resolution simulations coupling atomistic water to dissipative particle dynamics," *J. Chem. Phys.* **147** (11) (2017).
56. G. S. Ayton, H. L. Tepper, D. T. Mirijanian and G. A. Voth, "A new perspective on the coarse-grained dynamics of fluids," *J. Chem. Phys.* **120** (9), 4074-4088 (2004).
57. Y. Han, J. F. Dama and G. A. Voth, "Mesoscopic coarse-grained representations of fluids rigorously derived from atomistic models," *J. Chem. Phys.* **149**, 044104 (2018).
58. Y. Han, J. Jin and G. A. Voth, "Constructing many-body dissipative particle dynamics models of fluids from bottom-up coarse-graining," *J. Chem. Phys.* **154** (8), 084122 (2021).
59. J. J. Monaghan, "Smoothed particle hydrodynamics," *Annu. Rev. Astron. Astrophys.* **30** (1), 543-574 (1992).
60. J. J. Monaghan, "Smoothed particle hydrodynamics," *Mon. Not. R. Astron. Soc.* **68** (8), 1703 (2005).
61. J. J. Monaghan, "Smoothed particle hydrodynamics and its diverse applications," *Annu. Rev. Fluid Mech.* **44**, 323-346 (2012).
62. V. Ganesan and G. H. Fredrickson, "Field-theoretic polymer simulations," *Europhys. Lett.* **55**, 814 (2001).
63. G. H. Fredrickson, V. Ganesan and F. Drolet, "Field-Theoretic Computer Simulation Methods for Polymers and Complex Fluids," *Macromolecules* **35**, 16 (2002).
64. G. Fredrickson, *The equilibrium theory of inhomogeneous polymers*. (Oxford University Press, 2006).
65. L. D. Landau and E. M. Lifshitz, *Fluid Mechanics: Landau and Lifshitz: Course of Theoretical Physics, Volume 6*. (Elsevier, 2013).
66. H. C. Andersen and D. Chandler, "Optimized Cluster Expansions for Classical Fluids. I. General Theory and Variational Formulation of the Mean Spherical Model and Hard Sphere Percus-Yevick Equations," *J. Chem. Phys.* **57**, 1918 (1972).
67. D. Chandler and H. C. Andersen, "Optimized Cluster Expansions for Classical Fluids. II. Theory of Molecular Liquids," *J. Chem. Phys.* **57**, 1930 (1972).
68. H. C. Andersen, D. Chandler and J. D. Weeks, "Optimized Cluster Expansions for Classical Fluids. III. Applications to Ionic Solutions and Simple Liquids," *J. Chem. Phys.* **57**, 2626 (1972).
69. F. Hirata and P. J. Rossky, "An extended rism equation for molecular polar fluids," *Chem. Phys. Lett.* **83**, 329 (1981).
70. F. Hirata, B. M. Pettitt and P. J. Rossky, "Application of an extended RISM equation to dipolar and quadrupolar fluids," *J. Chem. Phys.* **77**, 509 (1982).

71. A. Kovalenko and F. Hirata, "Potentials of mean force of simple ions in ambient aqueous solution. I. Three-dimensional reference interaction site model approach," *J. Chem. Phys.* **112**, 10391 (2000).
72. A. Kovalenko and F. Hirata, "Potentials of mean force of simple ions in ambient aqueous solution. II. Solvation structure from the three-dimensional reference interaction site model approach, and comparison with simulations," *J. Chem. Phys.* **112**, 10403 (2000).
73. A. Kovalenko and F. Hirata, "Hydration free energy of hydrophobic solutes studied by a reference interaction site model with a repulsive bridge correction and a thermodynamic perturbation method," *J. Chem. Phys.* **113**, 2793 (2000).
74. D. Beglov and B. Roux, "Numerical solution of the hypernetted chain equation for a solute of arbitrary geometry in three dimensions," *J. Chem. Phys.* **103**, 360 (1995).
75. M. Doi and S. F. Edwards, *The theory of polymer dynamics*. (Oxford University Press, 1988).
76. F. S. Bates and G. H. Fredrickson, "Block copolymer thermodynamics: theory and experiment," *Annu. Rev. Phys. Chem.* **41** (1), 525-557 (1990).
77. G. H. Fredrickson and F. S. Bates, "Dynamics of block copolymers: Theory and experiment," *Annu. Rev. Mater. Sci.* **26** (1), 501-550 (1996).
78. F. Drolet and G. H. Fredrickson, "Combinatorial screening of complex block copolymer assembly with self-consistent field theory," *Phys. Rev. Lett.* **83** (21), 4317 (1999).
79. G. H. Fredrickson, V. Ganesan and F. Drolet, "Field-theoretic computer simulation methods for polymers and complex fluids," *Macromolecules* **35** (1), 16-39 (2002).
80. F. S. Bates, M. A. Hillmyer, T. P. Lodge, C. M. Bates, K. T. Delaney and G. H. Fredrickson, "Multiblock polymers: panacea or Pandora's box?," *Science* **336** (6080), 434-440 (2012).
81. M. C. Villet and G. H. Fredrickson, "Efficient field-theoretic simulation of polymer solutions," *J. Chem. Phys.* **141** (22), 224115 (2014).
82. K. T. Delaney and G. H. Fredrickson, "Recent developments in fully fluctuating field-theoretic simulations of polymer melts and solutions," *J. Phys. Chem. B* **120** (31), 7615-7634 (2016).
83. G. H. Fredrickson and K. T. Delaney, "Coherent states field theory in supramolecular polymer physics," *J. Chem. Phys.* **148** (20), 204904 (2018).
84. Y. Xuan, K. T. Delaney, H. D. Ceniceros and G. H. Fredrickson, "Machine learning and polymer self-consistent field theory in two spatial dimensions," *J. Chem. Phys.* **158** (14), 144103 (2023).
85. M. Kardar, *Statistical physics of fields*. (Cambridge University Press, 2007).
86. Y. Wang and G. A. Voth, "Unique spatial heterogeneity in ionic liquids," *J. Am. Chem. Soc.* **127** (35), 12192-12193 (2005).
87. D. Zubarev, "Computation of configuration integrals for a system of particles with Coulomb interaction," *Dokl. Akad. Nauk SSSR* **95**, 757-760 (1954).
88. L. Yukhnovsky, "Application of collective variables and taking account of short-range forces in a system of charged particles," *Zh. Eksp. Teor. Fiz.* **34** (2), 379-389 (1958).
89. J.-M. Caillol, O. Patsahan and I. Mryglod, "The collective variables representation of simple fluids from the point of view of statistical field theory," *Condens. Matter Phys.* **8** (2005).
90. J.-M. Caillol, O. Patsahan and I. Mryglod, "Statistical field theory for simple fluids: The collective variables representation," *Physica A* **368** (2), 326-344 (2006).

91. G. Parisi, *Statistical field theory*. (Addison–Wesley, Redwood City, 1988).
92. T. Ramakrishnan and M. Yussouff, “First-principles order-parameter theory of freezing,” *Phys. Rev. B* **19** (5), 2775 (1979).
93. D. W. Oxtoby, “Density functional methods in the statistical mechanics of materials,” *Annu. Rev. Mater. Res.* **32** (1), 39-52 (2002).
94. R. Wittkowski, H. Löwen and H. R. Brand, “Extended dynamical density functional theory for colloidal mixtures with temperature gradients,” *J. Chem. Phys.* **137** (22), 224904 (2012).
95. J. G. Anero, P. Español and P. Tarazona, “Functional thermo-dynamics: a generalization of dynamic density functional theory to non-isothermal situations,” *J. Chem. Phys.* **139** (3), 034106 (2013).
96. J. Hubbard, “Calculation of Partition Functions,” *Phys. Rev. Lett.* **3**, 77 (1959).
97. J. E. Hirsch, “Two-dimensional Hubbard model: Numerical simulation study,” *Phys. Rev. B* **31** (7), 4403 (1985).
98. G. V. Efimov and E. A. Nogovitsin, “The partition functions of classical systems in the Gaussian equivalent representation of functional integrals,” *Physica A* **234** (1-2), 506-522 (1996).
99. S. A. Baeurle, R. Martoňák and M. Parrinello, “A field-theoretical approach to simulation in the classical canonical and grand canonical ensemble,” *J. Chem. Phys.* **117**, 3027 (2002).
100. S. A. Baeurle, G. V. Efimov and E. A. Nogovitsin, “Calculating field theories beyond the mean-field level,” *Europhys. Lett.* **75**, 378 (2006).
101. S. A. Baeurle, G. V. Efimov and E. A. Nogovitsin, “On a new self-consistent-field theory for the canonical ensemble,” *J. Chem. Phys.* **124**, 224110 (2006).
102. S. A. Baeurle, “Method of Gaussian equivalent representation: a new technique for reducing the sign problem of functional integral methods,” *Phys. Rev. Lett.* **89** (8), 080602 (2002).
103. S. A. Baeurle, M. Charlot and E. A. Nogovitsin, “Grand canonical investigations of prototypical polyelectrolyte models beyond the mean field level of approximation,” *Phys. Rev. E* **75** (1), 011804 (2007).
104. E. Nogovitsyn, E. Gorchakova and M. Kiselev, “The Gaussian equivalent representation in thermodynamic self-consistent field theory,” *Russ. J. Phys. Chem. A* **81** (11), 1799-1803 (2007).
105. F. Schmid, “Self-consistent-field theories for complex fluids,” *J. Phys. Condens. Matter.* **10**, 8105 (1998).
106. M. W. Bates, J. Lequeieu, S. M. Barbon, R. M. Lewis III, K. T. Delaney, A. Anastasaki, C. J. Hawker, G. H. Fredrickson and C. M. Bates, “Stability of the A15 phase in diblock copolymer melts,” *Proc. Natl. Acad. Sci. U.S.A.* **116** (27), 13194-13199 (2019).
107. C. Zhang, D. L. Vigil, D. Sun, M. W. Bates, T. Loman, E. A. Murphy, S. M. Barbon, J.-A. Song, B. Yu and G. H. Fredrickson, “Emergence of hexagonally close-packed spheres in linear block copolymer melts,” *J. Am. Chem. Soc.* **143** (35), 14106-14114 (2021).
108. N. Sherck, K. Shen, M. Nguyen, B. Yoo, S. Kohler, J. C. Speros, K. T. Delaney, M. S. Shell and G. H. Fredrickson, “Molecularly informed field theories from bottom-up coarse-graining,” *ACS Macro Lett.* **10** (5), 576-583 (2021).
109. M. Nguyen, N. Sherck, K. Shen, C. E. Edwards, B. Yoo, S. Köhler, J. C. Speros, M. E. Helgeson, K. T. Delaney and M. S. Shell, “Predicting Polyelectrolyte Coacervation from a

- Molecularly Informed Field-Theoretic Model,” *Macromolecules* **55** (21), 9868-9879 (2022).
110. K. Shen, M. Nguyen, N. Sherck, B. Yoo, S. Köhler, J. Speros, K. T. Delaney, M. S. Shell and G. H. Fredrickson, “Predicting surfactant phase behavior with a molecularly informed field theory,” *J. Colloid Interface Sci.* **638**, 84-98 (2023).
 111. M. Nguyen, K. Shen, N. Sherck, S. Köhler, R. Gupta, K. T. Delaney, M. S. Shell and G. H. Fredrickson, “A molecularly informed field-theoretic study of the complexation of polycation PDADMA with mixed micelles of sodium dodecyl sulfate and ethoxylated surfactants,” *Eur. Phys. J. E* **46** (9), 75 (2023).
 112. A. Louis, P. Bolhuis, J. Hansen and E. Meijer, “Can polymer coils be modeled as “soft colloids”?,” *Phys. Rev. Lett.* **85** (12), 2522 (2000).
 113. J. Jin, J. Hwang and G. A. Voth, “Gaussian representation of coarse-grained interactions of liquids: Theory, parametrization, and transferability,” *J. Chem. Phys.* **159** (18), 184105 (2023).
 114. T. T. Foley, M. S. Shell and W. G. Noid, “The impact of resolution upon entropy and information in coarse-grained models,” *J. Chem. Phys.* **143** (24), 243104 (2015).
 115. J. F. Rudzinski and W. Noid, “Coarse-graining entropy, forces, and structures,” *J. Chem. Phys.* **135** (21), 214101 (2011).
 116. K. M. Kidder, R. J. Szukalo and W. Noid, “Energetic and entropic considerations for coarse-graining,” *The European Physical Journal B* **94** (7), 153 (2021).
 117. M. E. Johnson, T. Head-Gordon and A. A. Louis, “Representability problems for coarse-grained water potentials,” *J. Chem. Phys.* **126** (14) (2007).
 118. J. W. Wagner, J. F. Dama, A. E. Durumeric and G. A. Voth, “On the representability problem and the physical meaning of coarse-grained models,” *J. Chem. Phys.* **145** (4), 044108 (2016).
 119. N. J. H. Dunn, T. T. Foley and W. G. Noid, “Van der Waals perspective on coarse-graining: Progress toward solving representability and transferability problems,” *Acc. Chem. Res.* **49** (12), 2832-2840 (2016).
 120. J. Jin, A. J. Pak and G. A. Voth, “Understanding Missing Entropy in Coarse-Grained Systems: Addressing Issues of Representability and Transferability,” *J. Phys. Chem. Lett.* **10** (16), 4549-4557 (2019).
 121. T. Dannenhoffer-Lafage, J. W. Wagner, A. E. Durumeric and G. A. Voth, “Compatible observable decompositions for coarse-grained representations of real molecular systems,” *J. Chem. Phys.* **151** (13), 134115 (2019).
 122. W. G. Noid, J.-W. Chu, G. S. Ayton and G. A. Voth, “Multiscale coarse-graining and structural correlations: Connections to liquid-state theory,” *J. Phys. Chem. B* **111** (16), 4116-4127 (2007).
 123. W. L. Jorgensen, D. S. Maxwell and J. Tirado-Rives, “Development and testing of the OPLS all-atom force field on conformational energetics and properties of organic liquids,” *J. Am. Chem. Soc.* **118** (45), 11225-11236 (1996).
 124. L. S. Dodda, J. Z. Vilseck, J. Tirado-Rives and W. L. Jorgensen, “1.14* CM1A-LBCC: localized bond-charge corrected CM1A charges for condensed-phase simulations,” *J. Phys. Chem. B* **121** (15), 3864-3870 (2017).
 125. K. F. Freed, *Renormalization group theory of macromolecules*. (Wiley: New York, 1987).
 126. F. H. Stillinger, “Phase transitions in the Gaussian core system,” *J. Chem. Phys.* **65** (10), 3968-3974 (1976).

127. H. Yukawa, "On the interaction of elementary particles. I," *Proc. Phys. Math. Soc. Jpn.* **17**, 48-57 (1935).
128. T. Liverpool and M. Stapper, "The scaling behaviour of screened polyelectrolytes," *Europhys. Lett.* **40** (5), 485 (1997).
129. E. Y. Loh, J. E. Gubernatis, R. T. Scalettar, S. R. White, D. J. Scalapino and R. L. Sugar, "Sign problem in the numerical simulation of many-electron systems," *Phys. Rev. B* **41**, 9301 (1990).
130. T. D. Kieu and C. J. Griffin, "Monte Carlo simulations with indefinite and complex-valued measures," *Phys. Rev. E* **49**, 3855 (1994).
131. K. Schmidt and M. Kalos, in *Applications of the Monte Carlo Method in statistical physics* (Springer, 1984), pp. 125-143.
132. J. Jin, Y. Han and G. A. Voth, "A Field-Theoretical Paradigm via Hierarchical Coarse-Graining: II. Sampling, Estimators, and Multi-Component Systems," *J. Chem. Phys.* **Submitted** (2025).
133. J. A. Barker and D. Henderson, "Perturbation theory and equation of state for fluids. II. A successful theory of liquids," *J. Chem. Phys.* **47** (11), 4714-4721 (1967).
134. J. D. Weeks, D. Chandler and H. C. Andersen, "Role of repulsive forces in determining the equilibrium structure of simple liquids," *J. Chem. Phys.* **54** (12), 5237-5247 (1971).
135. J. Jin, K. S. Schweizer and G. A. Voth, "Understanding dynamics in coarse-grained models. I. Universal excess entropy scaling relationship," *J. Chem. Phys.* **158** (3), 034103 (2023).
136. J. Jin, K. S. Schweizer and G. A. Voth, "Understanding dynamics in coarse-grained models. II. Coarse-grained diffusion modeled using hard sphere theory," *J. Chem. Phys.* **158** (3), 034104 (2023).
137. J. Jin, E. K. Lee and G. A. Voth, "Understanding Dynamics in Coarse-Grained Models: III. Roles of Rotational Motion and Translation-Rotation Coupling in Coarse-Grained Dynamics," *J. Chem. Phys.* **159** (16), 164102 (2023).
138. J. Jin and G. A. Voth, "Understanding dynamics in coarse-grained models. IV. Connection of fine-grained and coarse-grained dynamics with the Stokes–Einstein and Stokes–Einstein–Debye relations," *J. Chem. Phys.* **161** (3) (2024).
139. J. Jin and G. A. Voth, "Understanding Dynamics in Coarse-Grained Models: V. Extension of Coarse-Grained Dynamics Theory to Non-Hard Sphere Systems," *arXiv preprint arXiv:2412.17186* (2024).
140. K. Singer, "Use of Gaussian Functions for Intermolecular Potentials," *Nature (London)* **181** (4604), 262-263 (1958).
141. B. B. Laird, J. Budimir and J. L. Skinner, "Quantum-mechanical derivation of the Bloch equations: Beyond the weak-coupling limit," *J. Chem. Phys.* **94** (6), 4391-4404 (1991).
142. J. Jin and D. R. Reichman, "Perturbative Expansion in Reciprocal Space: Bridging Microscopic and Mesoscopic Descriptions of Molecular Interactions," *J. Phys. Chem. B* **128** (4), 1061–1078 (2023).
143. B. Widom, "Intermolecular Forces and the Nature of the Liquid State: Liquids reflect in their bulk properties the attractions and repulsions of their constituent molecules," *Science* **157** (3787), 375-382 (1967).
144. J. Vera and J. Prausnitz, "Generalized van der Waals theory for dense fluids," *Chem. Eng. J.* **3**, 1-13 (1972).

145. S. I. Sandler, "The generalized van der Waals partition function. I. Basic theory," *Fluid Phase Equilib.* **19** (3), 238-257 (1985).
146. D. Beglov and B. Roux, "Solvation of complex molecules in a polar liquid: an integral equation theory," *J. Chem. Phys.* **104** (21), 8678-8689 (1996).
147. D. Beglov and B. Roux, "An integral equation to describe the solvation of polar molecules in liquid water," *J. Phys. Chem. B* **101** (39), 7821-7826 (1997).
148. A. Kovalenko and F. Hirata, "Three-dimensional density profiles of water in contact with a solute of arbitrary shape: a RISM approach," *Chem. Phys. Lett.* **290** (1-3), 237-244 (1998).
149. A. Kovalenko and F. Hirata, "Self-consistent description of a metal–water interface by the Kohn–Sham density functional theory and the three-dimensional reference interaction site model," *J. Chem. Phys.* **110** (20), 10095-10112 (1999).
150. L. Ornstein and F. Zernike, "The influence of accidental deviations of density on the equation of state," *Proc. Sect. Sci. K Ned. Akad. Wet.* **19** (2), 1312-1315 (1914).
151. K. S. Schweizer and J. G. Curro, "Integral-equation theory of the structure of polymer melts," *Phys. Rev. Lett.* **58** (3), 246 (1987).
152. K. S. Schweizer and J. G. Curro, "Integral equation theories of the structure, thermodynamics, and phase transitions of polymer fluids," *Adv. Chem. Phys.* **98**, 1-142 (1997).
153. F. Hirata, *Molecular theory of solvation*. (Springer Science & Business Media, 2003).
154. K. Schweizer and J. Curro, in *Atomistic Modeling of Physical Properties*, edited by L. Monnerie and U. W. Suter (Springer, Berlin, 1994), Vol. 116, pp. 319-377.
155. A. Jayaraman, in *Theory and Modeling of Polymer Nanocomposites*, edited by V. V. Ginzburg and L. M. Hall (Springer, 2021), pp. 1-22.
156. S. Boresch and M. Karplus, "The Jacobian factor in free energy simulations," *J. Chem. Phys.* **105** (12), 5145-5154 (1996).
157. M. J. Potter and M. K. Gilson, "Coordinate systems and the calculation of molecular properties," *The Journal of Physical Chemistry A* **106** (3), 563-566 (2002).
158. C.-E. Chang, M. J. Potter and M. K. Gilson, "Calculation of molecular configuration integrals," *J. Phys. Chem. B* **107** (4), 1048-1055 (2003).
159. B. J. Killian, J. Yundenfreund Kravitz and M. K. Gilson, "Extraction of configurational entropy from molecular simulations via an expansion approximation," *J. Chem. Phys.* **127** (2), 024107 (2007).
160. J. Jin and G. A. Voth, "Ultra-Coarse-Grained models allow for an accurate and transferable treatment of interfacial systems," *J. Chem. Theory Comput.* **14** (4), 2180-2197 (2018).
161. L. Martínez, R. Andrade, E. G. Birgin and J. M. Martínez, "PACKMOL: a package for building initial configurations for molecular dynamics simulations," *J. Comput. Chem.* **30** (13), 2157-2164 (2009).
162. S. Nosé, "A unified formulation of the constant temperature molecular dynamics methods," *J. Chem. Phys.* **81** (1), 511-519 (1984).
163. W. G. Hoover, "Canonical dynamics: equilibrium phase-space distributions," *Phys. Rev. A* **31** (3), 1695 (1985).
164. S. Plimpton, "Fast parallel algorithms for short-range molecular dynamics," *J. Comput. Phys.* **117**, 1-19 (1995).

165. W. M. Brown, P. Wang, S. J. Plimpton and A. N. Tharrington, “Implementing molecular dynamics on hybrid high performance computers—short range forces,” *Comput. Phys. Commun.* **182** (4), 898-911 (2011).
166. W. M. Brown, A. Kohlmeyer, S. J. Plimpton and A. N. Tharrington, “Implementing molecular dynamics on hybrid high performance computers—Particle—particle particle-mesh,” *Comput. Phys. Commun.* **183** (3), 449-459 (2012).
167. Y. Peng, A. J. Pak, A. E. Durumeric, P. G. Sahrman, S. Mani, J. Jin, T. D. Loose, J. R. Beiter and G. A. Voth, “OpenMSCG: A Software Tool for Bottom-up Coarse-graining,” *J. Phys. Chem. B* **127** (40), 8537-8550 (2023).